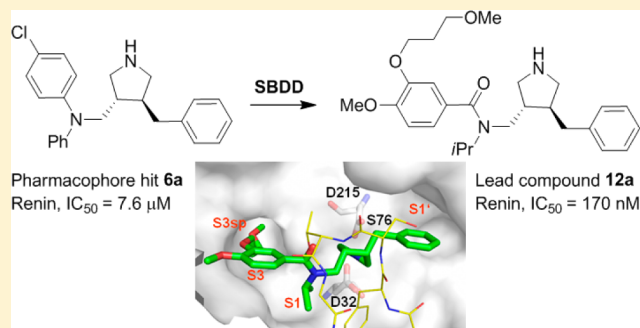


The Discovery of Novel Potent *trans*-3,4-Disubstituted Pyrrolidine Inhibitors of the Human Aspartic Protease Renin from in Silico Three-Dimensional (3D) Pharmacophore SearchesEdwige Lorthiois,^{*,†} Werner Breitenstein,[†] Frederic Cumin,[†] Claus Ehrhardt,[†] Eric Francotte,[†] Edgar Jacoby,[†] Nils Ostermann,[†] Holger Sellner,[†] Takatoshi Kosaka,^{‡,⊥} Randy L. Webb,[§] Dean F. Rigel,[§] Ulrich Hassiepen,[†] Paul Richert,[†] Trixie Wagner,[†] and Jürgen Maibaum^{*,†}[†]Novartis Pharma AG, Institutes for BioMedical Research, Novartis Campus, CH-4056 Basel, Switzerland[‡]Novartis Institutes for BioMedical Research, Ohkubo 8, Tsukuba, Ibaraki 300-2611, Japan[§]Novartis Pharmaceuticals Corp., Institutes for BioMedical Research, East Hanover, New Jersey, United States

jm301706j

Supporting Information

ABSTRACT: The small-molecule *trans*-3,4-disubstituted pyrrolidine **6a** was identified from in silico three-dimensional (3D) pharmacophore searches based on known X-ray structures of renin–inhibitor complexes and demonstrated to be a weakly active inhibitor of the human enzyme. The unexpected binding mode of the more potent enantiomer (3*S*,4*S*)-**6a** in an extended conformation spanning the nonprime and S1' pockets of the recombinant human (rh)-renin active site was elucidated by X-ray crystallography. Initial structure–activity relationship work focused on modifications of the hydrophobic diphenylamine portion positioned in S1 and extending toward the S2 pocket. Replacement with an optimized P3–P1 pharmacophore interacting to the nonsubstrate S3^{sp} cavity eventually resulted in significantly improved in vitro potency and selectivity. The prototype analogue (3*S*,4*S*)-**12a** of this new class of direct renin inhibitors exerted blood pressure lowering effects in a hypertensive double-transgenic rat model after oral administration.



INTRODUCTION

Chronic elevation of systemic blood pressure, known as hypertension, is an important risk factor for cardiovascular disease such as congestive heart failure, stroke, and myocardial infarction and is the leading cause of death in the western world.¹ The renin–angiotensin–aldosterone system (RAAS)² plays a fundamental role in normal blood pressure control and body fluid volume homeostasis, while excessive stimulation of the RAAS contributes directly to cardiorenal diseases.³ The highly substrate-specific aspartic protease renin found in the circulation following synthesis and release from juxtaglomerular cells of the kidney⁴ catalyzes the first and rate limiting cleavage step of the RAAS, generating the biologically inactive decapeptide angiotensin I (AngI) from the α₂-globulin angiotensinogen substrate.⁵ AngI is further processed by the angiotensin-converting enzyme (ACE) to generate the octapeptide AngII. The interaction of AngII with the AT1 receptor triggers various hemodynamic effects, such as sodium and water retention, stimulation of aldosterone release, and potent vasoconstriction.⁶ Furthermore, AngII exerts direct growth factor-like effects via several pathways mainly downstream of AT1 inducing cell proliferation or fibrosis.⁷ Direct

renin inhibitors (DRIs) may provide unique therapeutic benefits^{5,8–11} as a result of more complete blockade of the RAAS at source by preventing the formation of AngI and AngII at compensatory elevated circulating renin levels and hence the formation of AngI derived products¹² without affecting kinin metabolism.¹³ Moreover, clinical studies have demonstrated the potential of direct renin inhibition for end organ protection beyond blood pressure lowering effects.¹⁴

Our current perspective on designing orally active DRIs has experienced a remarkable transformation during more than three decades starting from peptide-like transition-state inhibitors and subsequently progressing toward various distinct classes of nonpeptide inhibitors (**1–4**, Figure 1).^{15,16} Inhibitor **1** (aliskiren, Tekturna, Rasilez) has received recently marketing approval as the first DRI for the treatment of hypertension. The compound has emerged from a S₃–S₁ topological design concept, which notably exploited in addition tight binding interactions to the nonsubstrate S₃ subpocket (S₃^{sp}) of human renin.^{17,18} The early class of 3,4-piperidine-based “group

Received: November 20, 2012

Published: February 20, 2013

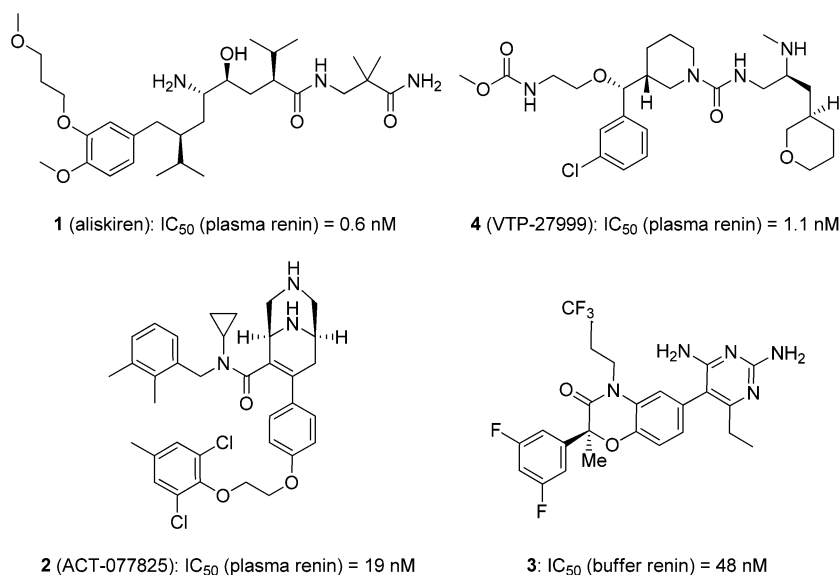


Figure 1. Diverse classes of nonpeptide direct inhibitors.

replacement assisted binding (GRAB) peptidomimetics”,¹⁹ first reported by Hoffmann-La Roche,^{20,21} has further advanced to 3,9-diazabicyclo[3.3.1]nonenes, such as **2** (ACT-077825) (Figure 1), which has undergone phase II clinical trials.²² The basic amine mono- or bicyclic center scaffolds of such GRAB peptidomimetic inhibitors form favorable charge-enforced H-bond interactions to the catalytic Asp₃₂ and Asp₂₁₅. More intriguingly, these DRIs bind to a fundamentally different enzyme active site topography characterized by an open conformation of the flap β -hairpin and formation of a large hydrophobic pocket (Tyr₇₅ flap pocket) that is unrecognized by the renin substrate. A series of potent 2,4-diaminopyrimidines, such as **3**, bearing a P₃-P₁ benzoxazinone pharmacophore and interacting with the basic heterocyclic headgroup to the catalytic dyad, have been reviewed elsewhere.^{16,23} Most recently, the alkylamine class of DRIs has attracted much interest with compound **4** (VTP-27999) (Figure 1) having been reported to be under clinical investigation.²⁴

We have embarked on a broad integrated screening program encompassing multiple approaches in parallel in the quest for identifying attractive novel-class druglike scaffolds, potentially leading to orally efficacious DRIs with improved oral bioavailability and reduced cost of goods. These efforts included two large-scale HTS campaigns using both an enzymatic and a competitive ligand binding assay format, a combined NMR/X-ray fragment-based screen of an aspartic protease-family directed library, as well as virtual searches utilizing the renin-inhibitor X-ray structure knowledge. The various screening approaches that were utilized proved to be remarkably complementary in identifying attractive hits of high structural diversity from different sources.²⁵ We report herein the discovery of the novel 3,4-disubstituted pyrrolidine **6** from a computational pharmacophore search and our initial SAR work guided by X-ray crystallography, leading to the orally active (3*S*,4*S*)-**12a** with significantly improved potency and selectivity.

RESULTS AND DISCUSSION

A virtual screening approach was developed based on three-dimensional (3D) pharmacophore models constructed from the X-ray crystal structures of renin-inhibitor complexes representing a diversity of active site binding topographies,

followed by Unity 3D flexible pharmacophore searching within the Novartis compound database.^{26a} The selected X-ray complexes included that of the low-affinity *trans*-3,4-piperidine **5**²⁷ (34% inhibition of rh-renin at 10 μ M concentration in the FRET enzymatic assay;^{26a} Figures 2 and 3), which was resolved

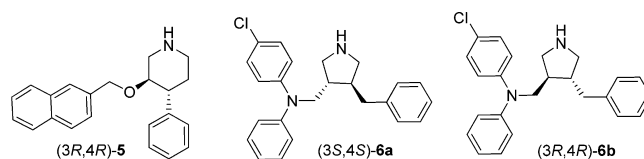


Figure 2. *trans*-3,4-Piperidine (3*R*,4*R*)-**5** used for 3D pharmacophore search and pharmacophore hit **6**.

in our group at 2.4 Å resolution.^{26a} In brief, the key elements of the three-point pharmacophore derived from (3*R*,4*R*)-**5** were

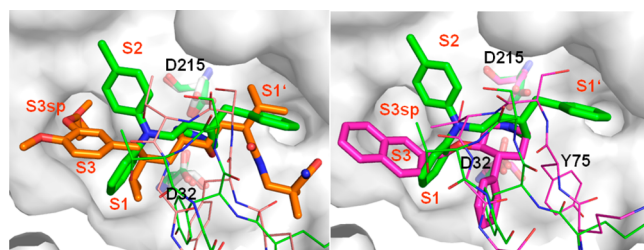


Figure 3. X-ray crystal structure of the *trans*-3,4-pyrrolidine **6a** (shown as stick model in green color) bound to the active site of glycosylated rh-renin (refined at 2.6 Å resolution) and superimposed with inhibitor **1** (left-hand side picture; orange color; PDB code 2V0Z)^{17b,28} and inhibitor **5** (right-hand side picture; magenta color) in complex with rh-renin. Shown is the solvent accessible surface of renin. Residues of the flap β -hairpin (residues Tyr₇₅, Ser₇₆, Thr₇₇, and Gly₇₈) are depicted as thin lines in green, orange, and magenta for the rh-renin/**6a**, rh-renin/**1**, and rh-renin/**5** complexes, respectively, and have been omitted from the protein surface calculation. The oxygen and nitrogen atoms of the ligands are colored in red and blue, respectively. The absolute (3*S*,4*S*)-configuration of **6a** was tentatively assigned based on the observed difference electron density and was subsequently confirmed by synthesis and chemical correlation with an authentic sample (see text for discussion).

defined by the basic piperidine nitrogen atom interacting to the catalytic Asp₃₂ and Asp₂₁₅, the geometric center of the S₃–S₁ binding naphthyl, and of the C4 phenyl residue positioned in the Tyr₇₅ flap pocket. Both hydrophobic centers were defined with a positional constraint of 1.5 Å.

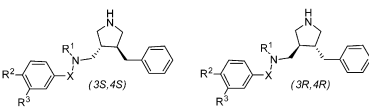
The primary in silico hit list comprising a total of 3717 compounds was further refined by adding Unity volume constraints for the van der Waals surfaces of the protein atoms calculated with MOLCAD.^{26a} The surface constraints were generated and applied independently by using both the X-ray crystal complex structure of **5** and that of a related analogue bearing an extended *ortho*-chlorobenzylloxymethyl moiety at the C4' phenyl position (PDB code 1PR8).²⁰ Triaging by visual inspection of the combined remaining hits removed compounds with an apparent structural alert, and physical availability in the corporate database was then checked. A total of 328 compounds were finally tested for renin inhibition using a fluorescence resonance energy transfer (FRET) biochemical assay identifying four weakly active nonpeptide hits. (*Rac*)-**6** was the most potent, with an IC₅₀ of 14 μM (Figure 2, Table 1), representing the first attractive analogue of

phenyl of piperidine **5**, as was anticipated from the 3D pharmacophore search and suggested by additional modeling work. The basic pyrrolidine nitrogen atom of **6a** occupied the pivotal position almost symmetrical between the catalytic Asp₃₂ and Asp₂₁₅ of renin, as was predicted by modeling, most likely forming electrostatically enforced H-bond interactions to both carboxylates. The very close superposition of the five-membered ring transition-state surrogate of **6a** with the center piperidine scaffold of renin-bound **5** was quite noteworthy.

The difference electron density map observed for **6a** was only compatible with absolute (3*S*,4*S*)-configuration. The ligand was bound in an energetically less favored trans-pseudoaxial conformation which allowed the hydrophobic 3(*S*)-benzyl residue to be positioned in the S₁' pocket in an unusual orientation almost perpendicular to the axis of this binding site (Figure 3). Interestingly, a significant conformational movement of Pro₂₉₂ toward the phenyl C4 of **6a** was noted. On the other hand, the lipophilic *N,N*-diphenylamino moiety was bound to the nonprime site with the unsubstituted *N*-phenyl interacting with S₁ pocket. The *N*-4-chlorophenyl was located at the entrance of the S₂ pocket of rh-renin and in close distance to Ser₂₁₉, with the chlorine atom pointing toward the aryl side chain of Tyr₂₂₀ within 3.4 Å binding distance. The 4-chlorophenyl portion nicely overlapped with the P₃/P₂ carboxamide group of peptide-like peptidomimetic DRIs²⁸ in a perpendicular relative conformation. Notably, the closed flap β-hairpin adopted a significantly different conformation as was observed for the S₃–S₁ topological inhibitor **1** (Figure 2). This was attributed to the fact that a second molecule of **6a** was observed in the crystal structure, binding to the S₃ and S₄ nonprime sites with the chlorophenyl residue being in close contact with the flap region and forming a direct H-bond interaction to the side chain of Tyr₂₂₀ via its pyrrolidine nitrogen. Two entities of renin were present in the asymmetric unit of the crystal, each complexed with two molecules of inhibitor **6a**. The unsubstituted phenyl ring of each “second site” inhibitor molecules was engaged in intermolecular contacts with the Phe₂₄₂ side chains of both renin entities in the crystal packing.^{26c} Interestingly, the electron density was well-defined and the inhibitor occupancy was identical for both ligands binding to the active site of renin in the S₁' and S₂ or the S₃ and S₄ nonprime sites, respectively. On the basis of these observations, a significant contribution of the second ligand to the binding affinity of **6a** to the S₁'/S₂ active site cannot be ruled out. Quantification of the energetic contributions of the “second ligand” would require additional experiments.

Retrospectively, the 3D pharmacophore-assisted discovery of **6a** as a weakly active inhibitor of human renin is quite remarkable in view of its unexpected binding pose unveiled by X-ray crystallography. The two hydrophobic constraints in combination with the basic amine constraint of our pharmacophore model derived from the GRAB peptidomimetic **5** were fully matched by the two aromatic substituents of the *N,N*-diphenylamino moiety and the pyrrolidine template of **6a**, respectively. In this model, the unsubstituted *N*-phenyl moiety of **6a** matched with the C4 phenyl group of **5** binding to the open-flap conformation, and the *N*-*para*-Cl-phenyl corresponded to the S₁–S₃ naphthalene scaffold of **5**. Notably, the exclusion volume derived from the published X-ray structure (1PR8) of a GRAB peptidomimetic binding deeply into the open flap pocket accommodated **6** in its pharmacophore-derived orientation and conformation. On the other hand, there was not sufficient space within the exclusion volume derived

Table 1. In Vitro Inhibition of rh-Renin^a

Cpd ^b	Absolute stereochemistry					IC ₅₀ , μM ^a
		R ¹	X	R ²	R ³	
6	(3 <i>S</i> ,4 <i>S</i>)/(3 <i>R</i> ,4 <i>R</i>) ^c	4-ClPh	-	H	H	14
6a	(3 <i>S</i> ,4 <i>S</i>)	4-ClPh	-	H	H	7.6
6b	(3 <i>R</i> ,4 <i>R</i>)	4-ClPh	-	H	H	18
7	(3 <i>S</i> ,4 <i>S</i>)/(3 <i>R</i> ,4 <i>R</i>) ^c	4-ClPh	CH ₂	H	H	4.1
8	(3 <i>S</i> ,4 <i>S</i>)/(3 <i>R</i> ,4 <i>R</i>) ^c	4-ClPh	CH ₂	OMe	O(CH ₂) ₃ OMe	9.8
9	(3 <i>S</i> ,4 <i>S</i>)/(3 <i>R</i> ,4 <i>R</i>) ^c	iPr	CH ₂	OMe	O(CH ₂) ₃ OMe	7.7
10	(3 <i>S</i> ,4 <i>S</i>)/(3 <i>R</i> ,4 <i>R</i>) ^c	4-ClPh	CO	OMe	O(CH ₂) ₃ OMe	1.7
11	(3 <i>S</i> ,4 <i>S</i>)/(3 <i>R</i> ,4 <i>R</i>) ^c	Ph	CO	OMe	O(CH ₂) ₃ OMe	1.9
12	(3 <i>S</i> ,4 <i>S</i>)/(3 <i>R</i> ,4 <i>R</i>) ^c	iPr	CO	OMe	O(CH ₂) ₃ OMe	0.45
12a	(3 <i>S</i> ,4 <i>S</i>)	“	“	“	“	0.17
12b	(3 <i>R</i> ,4 <i>R</i>)	“	“	“	“	2.7

^aHalf-maximal inhibition of rh-renin determined in a FRET-based enzymatic assay using (RE(EDANS)IHPFHLVIHTK(Dabcyl)R as the substrate in 100 mM Tris–HCl buffer pH 7.4.^{26a} Data represent mean values from duplicates. ^bAll compounds prepared as HCl salts. ^cRacemic mixture.

a new chemotype DRI. Racemic resolution of **6** by chiral HPLC (Chiracel OD) afforded the single enantiomer **6a** (enantiomeric excess *ee* >99.9%), with an IC₅₀ of 7.6 μM toward rh-renin and being slightly more potent compared to its antipode **6b** (IC₅₀ = 18 μM, Table 1). Also, compound **6a** only weakly inhibited other human aspartic proteases with IC₅₀ = 11 μM for both rh-cathepsin D and E and IC₅₀ = 4.5 and 29 μM for rh-pepsin A and C, respectively. The absolute configuration of (3*S*,4*S*)-**6a** was subsequently confirmed by synthesis and chemical correlation with an authentic sample (*vide infra*).^{26b}

We were very gratified that the X-ray crystal structure of the weakly active **6a** in its complex with rh-renin could be rapidly resolved by the soaking method,^{26a} revealing an unexpected ligand binding orientation along the axis of the enzyme substrate cleft (Figure 3). In its complex, **6a** adopted an extended conformation spanning both the prime and nonprime recognition sites. Most notably, **6a** lacked any binding interaction to the open flap Tyr₇₅ pocket similar to the C4

from the human renin/5 crystal complex structure because the open-conformation flap pocket in this case was too narrow in order to identify **6** as a potential ligand of the enzyme.

The insight gained by X-ray crystallography into the binding interactions of (3*S*,4*S*)-**6a** was crucial for developing an efficient hit-to-lead optimization strategy. Initially, we focused our attention on exploring the potential offered by the unprecedented *N,N*-diphenylamine nonprime site binding motif to improve the binding affinity to rh-renin. Specifically, major efforts addressed modifications of the “upper” *N*-4-chlorophenyl portion with the aim to induce a H-bond to the Ser₂₁₉ at the entrance of the nonsubstrate S₃^{SP} cavity and/or to tether this aryl portion by a short linker and to further expand into the unoccupied S₂ pocket. Combined attempts were also made to fill the large hydrophobic S₃–S₁ pocket by appropriately substituting the S₁ binding *N*-phenyl residue. However, while more than 150 analogues of **6** with such modifications of both *N*-aryl groups were synthesized, no significant improvement in potency was accomplished (data not shown).

The superimposed X-ray crystal structures of (3*S*,4*S*)-**6a** and **1**^{17,28} revealed the *N,N*-diphenylamine nitrogen atom of **6a** to be positioned very closely to the chirality center bearing the S₁ isopropyl group of **1** (Figure 3). This prompted us to merge the unique key structural elements of both inhibitor chemotypes by combining the optimized topological P₃/P₃^{SP}–P₁ pharmacophore of **1** with the 3,4-pyrrolidine center transition-state surrogate of **6a**. Analogues of **1** bearing either a basic *N*-isopropyl tertiary amine or the related neutral *N*-isopropyl benzamide P₃–P₁ motif had been previously discovered to display high in vitro potency toward human renin.²⁹ Compounds (*rac*)-**7** and (*rac*)-**8** in which the *N*-phenyl of **6** is replaced by an unsubstituted benzyl and a P₃^{SP}-tethered dialkoxybenzyl group, respectively, were found to be equipotent to (3*S*,4*S*)-**6a** (Table 1). Furthermore, the *N*-isopropyl analogue (*rac*)-**9** surprisingly did not show improved inhibitory affinity in the FRET biochemical assay.

Next, we investigated the introduction of a carbonyl linker in order to avoid a basic amine functional group at P₁ and to constrain the ligand conformational flexibility. In addition, computational docking predicted a H-bond interaction between the spacer carbonyl and Thr₇₇ of the flap β -hairpin,²⁹ anticipating a closed binding conformation similar to that of the renin–inhibitor **1** complex. A ~5-fold improvement in potency was observed for the *N*-chlorophenyl-*N*-benzamide (*rac*)-**10** (IC₅₀ = 1.7 μ M) and its *des*-chloro analogue (*rac*)-**11** (Table 1). Most notably, a further significant increase in inhibitory affinity was accomplished with the *N*-isopropyl analogue (*rac*)-**12** (IC₅₀ = 0.45 μ M). This result was considered to be in line with previous findings³⁰ indicating that the *N*-phenyl residue would be suboptimal for this inhibitor series to be smoothly accommodated by the S₁ pocket. The pure enantiomer (3*S*,4*S*)-**12a** showed an IC₅₀ of 170 nM and was 15 times more active compared to the distomer (3*R*,4*R*)-**12b** (Table 1). Importantly, the potency of (3*S*,4*S*)-**12a** toward renin was retained when measured in the presence of human plasma (IC₅₀ = 300 nM). Furthermore, (3*S*,4*S*)-**12a** was highly selective against human pepsins A, C, human cathepsins D, E, as well as human BACE-1 and BACE-2 (all IC₅₀ > 30 μ M).

The X-ray crystal structure of (3*S*,4*S*)-**12a** in complex with rh-renin (Figure 4) revealed a strikingly close overlay of the 3,4-dialkoxy phenyl portion accommodated by the S₃–S₃^{SP} cavity and of the S₁ *N*-isopropyl group with the respective

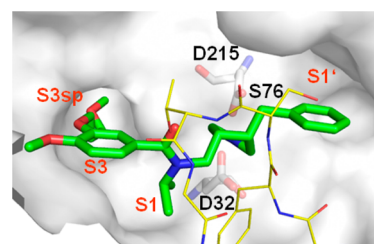


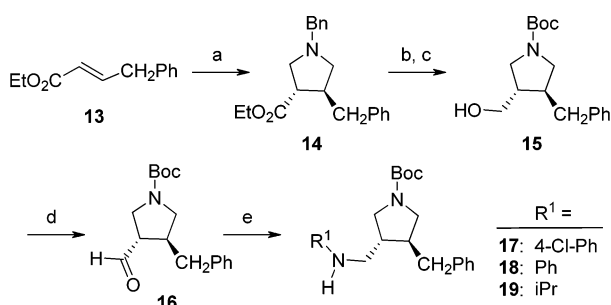
Figure 4. X-ray crystal structure of (3*S*,4*S*)-**12a** (shown as stick model in green color) bound in the rh-renin active site (2.8 Å resolution), see Experimental Section. Shown is the solvent accessible surface of the active site of rh-renin. Residues of the flap β -hairpin are depicted in yellow as thin lines and have been omitted for protein surface calculation. The catalytic aspartates are shown as stick models. Oxygen and nitrogen atoms are shown in red and blue color, respectively.

pharmacophore residues of inhibitor **1**. The methoxypropyloxy side chain of **12a** was bound in an extended conformation into the nonsubstrate S₃^{SP} channel of rh-renin, forming an H-bond between the distal ether oxygen and the NH of the Tyr₁₄ backbone, while the *para*-methoxy group fills the S₃ pocket. The *N*-isopropyl of **12a** was penetrating more deeply into S₁ compared to the *N*-phenyl of (3*S*,4*S*)-**6a**,³⁰ thereby forming closer van der Waals contacts to the hydrophobic surface of this pocket. The benzamide moiety of **12a** was bridging the contiguous S₃–S₁ “superpocket” by adopting a distorted conformation in which the carbonyl group is rotated by a 90° angle relative to the plane of the phenyl portion. In addition, the carbonyl of the P₃–P₁ carboxamide spacer was in H-bond distance (2.8 Å) to the hydroxyl of the flap Thr₇₇ residue.²⁹ The flap β -hairpin loop was in a closed conformation with the backbone and side chains of Tyr₇₅–Ser₇₆–Thr₇₇–Gly₇₈, being in a very similar orientation as observed for inhibitor **1**. The only major difference was found for the hydroxyl group of Ser₇₆, which was flipped toward solvent space in the case of rh-renin bound **6a**. On the other hand, the center pyrrolidine scaffold as well as the hydrophobic 3(*S*)-benzyl group binding to the S₁' site of both **12a** and the initial hit **6a** (Figure 4) were in a virtually identical position within the rh-renin active cleft. Interestingly, the basic pyrrolidine nitrogen atom of **12a** was located almost symmetrically between the primary amine NH₂ and the hydroxyl group of the aminohydroxyethylene dipeptide isostere of **1**, forming a H-bond network to the catalytic dyad which is partially distinct from that of classical hydroxyethylene (HE) isosteres of peptide-derived peptidomimetics.²⁸

With the discovery of the 3,4-piperidine based GRAB peptidomimetic renin inhibitors, basic cyclic secondary amine skeletons have been recognized as privileged core structural entities interacting with the enzyme family specific catalytic dyad for the conceptual design of novel aspartic protease inhibitors.^{20,31–34} The five-membered 3,4-di(aminomethyl)-pyrrolidine template has been utilized for the design of potent HIV-1 protease inhibitors as well as for cathepsin D and was predicted by modeling to bind into the S₂–S₂' specificity pockets.³¹ X-ray crystallography confirmed the basic pyrrolidine nitrogen atom to be positioned in close binding distance to both catalytic aspartates of the HIV protease and, most notably, unveiled an unexpected inhibitor pose characterized by an altered occupation of the recognition pockets and a major conformational distortion of the flap region.³¹ 3,4-Trisubstituted pyrrolidine-based BACE-1 inhibitors have been reported recently and were demonstrated by X-ray crystallography to

form a bidentate interaction between the pyrrolidine nitrogen and the two aspartate residues from the catalytic dyad.³⁵ Notably, the spiro-tetrahydronaphthalene moiety in position 4 binding in the S_1 pocket and the 2,4-diphenyl substituted piperidine moiety attached to the C3 occupied a newly formed pocket under the flap with one phenyl group pointing toward the S_2' pocket.³⁵ The *trans*-3,4-pyrrolidine **12a** reported herein represents the first prototype of a new class of DRIs that interacts to the extended β -strand substrate binding topography with the flap β -hairpin in a closed conformation and by spanning the S_3 - S_1' specificity pockets in a topological fashion.³⁶

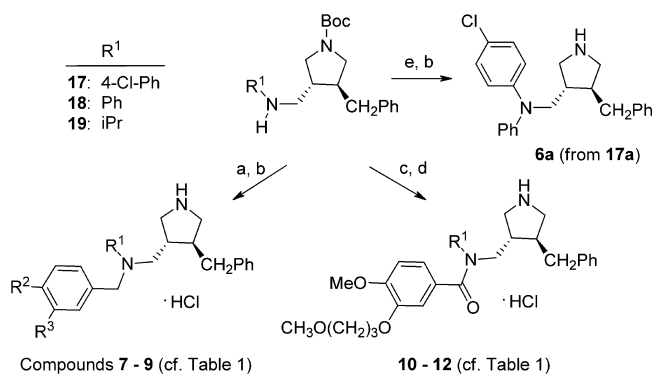
An efficient synthesis of the key *trans*-pyrrolidine-3-carbaldehyde intermediate (*rac*)-**16** was established as outlined in Scheme 1, providing flexible access to various nonprime side

Scheme 1^a

^a(a) *N*-Benzyl-*N*-(methoxymethyl)trimethylsilyl methylamine, TFA, toluene, 0°C, 88%; (b) H_2 , Pd(OH)₂, (Boc)₂O, EtOH, RT, 95%; (c) LiBH₄, THF, reflux, 60%; (d) Dess–Martin periodinane, wet CH₂Cl₂, 89%; (e) R¹-NH₂, NaBH(OAc)₃, 1,2-dichloroethane, RT.

chain modifications. Ethyl *trans*-4-phenyl-2-butenolate **13** readily obtained from phenylacetaldehyde by Wittig–Horner olefination was converted via a 1,3-dipolar cycloaddition reaction to afford the *trans*-configured pyrrolidine (*rac*)-**14**.^{26b} Reductive debenzoylation and in situ *N*-Boc protection followed by LiBH₄ reduction of the ester furnished the alcohol derivative (*rac*)-**15**. Dess–Martin oxidation to the aldehyde (*rac*)-**16** was followed by reductive amination to afford the secondary amine derivatives (*rac*)-**17** to (*rac*)-**19**, respectively. Inhibitors (*rac*)-**7** to (*rac*)-**9** were prepared from (*rac*)-**17** or (*rac*)-**19** by *N*-alkylation with the respective benzyl bromides in the presence of K₂CO₃ or by reductive amination using 4-methoxy-3-(3-methoxypropoxy)-benzaldehyde/NaBH(OAc)₃, followed by removal of the *N*-Boc protecting group (Scheme 2). *N*-Acylation of amines (*rac*)-**17** to (*rac*)-**19** with 4-methoxy-3-(3-methoxypropoxy)-benzoylchloride and final deprotection afforded inhibitors (*rac*)-**10**, (*rac*)-**11**, and (*rac*)-**12**, respectively (Scheme 2).

Resolution of the alcohol intermediate (*rac*)-**15** was accomplished by preparative chiral HPLC (Chiracel OJ) to afford the single enantiomers (3*S*,4*S*)-**15a** and (3*R*,4*R*)-**15b** with high enantiomeric excess of *ee* ≥ 99.8%. The absolute configuration of both (3*S*,4*S*)-**15a** and (3*R*,4*R*)-**15b** was unambiguously assigned by their transformation to the crystalline aniline derivatives (3*S*,4*R*)-**17a** and (3*R*,4*S*)-**17b** according to Scheme 1 and subsequent X-ray diffraction analysis.^{26a} Intermediate (3*S*,4*R*)-**17a** served as starting material for the preparation of the pure enantiomer (3*S*,4*S*)-**6a** according to Scheme 2, thereby confirming the initially tentative assignment of the absolute configuration of rh-renin

Scheme 2^a

^a(a) R-CH₂Br, K₂CO₃, DMF, 80°C or 4-methoxy-3-(3-methoxypropoxy)-benzaldehyde, NaBH(OAc)₃, 1,2-dichloroethane, RT; (b) TFA, CH₂Cl₂ and formation of HCl salt,^{26b} or 4 M HCl–dioxane; (c) 4-methoxy-3-(3-methoxypropoxy)-benzoylchloride, Et₃N, CH₂Cl₂, RT; (d) HCl–*i*PrOH, RT; (e) [Pd(μ-Br)(*t*-Bu₃P)]₂, *t*BuOK, PhBr, toluene 110 °C.

bound **6a** as determined by X-ray crystallography (vide supra). Furthermore, both enantiomeric inhibitors (3*S*,4*S*)-**12a** and (3*R*,4*R*)-**12b** were prepared from (3*S*,4*S*)-**15a** and (3*R*,4*R*)-**15b**, respectively, according to Scheme 2.

To further assess the lead potential of the prototype inhibitor (3*S*,4*S*)-**12a**, the in vitro selectivity against a broad safety pharmacology panel of receptors and ion channels, the pharmacokinetic profile in rat and the in vivo efficacy in hypertensive double-transgenic rats (dTGRs) overexpressing both human renin and human angiotensinogen³⁷ were evaluated. (3*S*,4*S*)-**12a** was found to be inactive against 52 receptors (all IC₅₀ >10 μM) and only weakly active against 5-HT_{1A}, 2A, 2B, and the α₁-adrenoceptor (IC₅₀s ranging between 1 and 10 μM), respectively. The compound had modest affinity to the hERG channel with IC₅₀ = 14.5 μM (mean value from two independent measurements using an in vitro dofetilide binding assay). Absolute oral bioavailability was 53% in cannulated fed Sprague–Dawley rats when dosed at 2 mg/kg intravenously and 6 mg/kg orally (estimated *t*_{1/2} = 2 h; Cl_p = 1.5 L/h/kg; V_{dss} = 2.8 L/kg; oral C_{max} = 1310 nM; oral AUC_(0–24 h) = 4810 nM·h). Single oral dosing of (3*S*,4*S*)-**12a** to telemetered dTGRs at 6 and 30 mg/kg resulted in a dose-dependent moderate reduction in mean arterial blood pressure (MAP) with peak changes in MAP of 15 and 35 mmHg, respectively. Blood pressure returned to baseline pretreatment levels after 12 h, demonstrating a sustained pharmacological effect of the compound in this model.

CONCLUSION

In summary, a small-molecule *trans*-3,4-disubstituted pyrrolidine derivative was discovered from an in silico 3D pharmacophore approach as a weakly active screening hit toward rh-renin. Utilizing X-ray crystal structure information, the combination of the center basic amine transition-state surrogate with an optimized P₃/P₃^{SP}-P₁ scaffold derived from **1** resulted in (3*S*,4*S*)-**12a** with submicromolar in vitro potency. The druglike lead compound of a novel class of DRIs demonstrated promising pharmacokinetic and pharmacodynamic properties in rat. Results from continued work focusing on prime site modifications and leading to highly potent clinical candidates will be presented in due course.

EXPERIMENTAL SECTION

Chemistry General Procedures. Unless otherwise specified, all solvents and reagents were obtained from commercial suppliers and used without further drying or purification. Normal-phase flash chromatography was performed using Merk silica gel 60 (230–400 mesh). R_f values for TLC are measured on 5 cm × 10 cm TLC plates, silica gel F₂₅₄, Merck, Darmstadt, Germany. Purity was determined by analytical HPLC from the integration of the area under the UV absorption curve at $\lambda = 254$ or 214 nm signals. ^1H NMR and ^{13}C NMR spectra were recorded on a Bruker DPX400 BBO spectrometer and a Bruker Avance 600 spectrometer using a ^{13}C – ^1H dual cryoprobe. ^1H and ^{13}C NMR spectra were recorded at 394 K on a Bruker DPX400 TXI spectrometer. Chemical shift (δ) values were referenced to tetramethylsilane as internal standard and are reported in parts per million (ppm). Mass spectral HRMS were obtained using electrospray ionization in positive ion modus. The elemental composition was derived from the averaged mass spectra acquired at the high resolution of about 30000 on an 9.4T APEX-III FT-MS (Bruker Daltonics). The high mass accuracy below 1 ppm was obtained using an internal calibration.

Preparation of Intermediates 13, 14, 15(a,b), 16, 17(a,b), 19(a,b). (*E*-4-Phenyl-but-2-enoic Acid Ethyl Ester (13). To a solution of triethylphosphonoacetate (9.00 mL, 45.4 mmol) in THF (90 mL) was added sodium hydride (60% dispersion in oil, 1.81 g, 45.4 mmol) at RT under an N_2 atmosphere. The reaction mixture was stirred at 25 °C for 45 min, and phenylacetaldehyde (4.87 mL, 41.0 mmol) was added. After 30 min at RT, the reaction was partitioned between Et_2O and water. The aqueous layer was extracted three times with Et_2O , dried over Na_2SO_4 , filtered, and concentrated. The crude material was purified by flash chromatography on silica gel (eluent: *c*-hexane–EtOAc 90:10) to give 13 (7.0 g, 81%) as a colorless oil. TLC, R_f (*c*-hexane–EtOAc 90:10) = 0.55. MS (LC-MS): 191.0 [M + H]⁺. t_R (HPLC, Waters Symmetry C18, 3.5 μm , 2.1 mm × 50 mm, 20–95% CH_3CN – H_2O /3.5 min, 95% CH_3CN /2 min, CH_3CN and H_2O containing 0.1% TFA; flow, 0.6 mL/min): 3.6 min. ^1H NMR (DMSO- d_6 , 400 MHz): δ 1.17 (t, $J = 7.1$ Hz, 3H), 3.53 (dd, $J = 7.0$, 1.3 Hz, 2H), 4.08 (q, $J = 7.1$ Hz, 2H), 5.83 (dt, $J = 15.6$, 1.3 Hz, 1H), 6.97 (dt, $J = 15.6$, 7.0 Hz, 1H), 7.20–7.24 (m, 3H), 7.30–7.33 (m, 2H).

(3*S*,4*S**)-1,4-Dibenzyl-pyrrolidine-3-carboxylic Acid Ethyl Ester ((*rac*)-14). To a stirred solution of 13 (4.70 g, 24.7 mmol) in toluene (60 mL) was added *N*-benzyl-*N*-(methoxymethyl)trimethylsilylamine (6.54 mL, 25.6 mmol) at 0 °C under an N_2 atmosphere. Trifluoroacetic acid (0.19 mL, 2.47 mmol) was added at 0 °C, and the mixture was stirred for 30 min at RT overnight.³⁸ The reaction was quenched by addition of a saturated aqueous solution of NaHCO_3 and was the extracted three times with EtOAc. The combined organics were dried over Na_2SO_4 and concentrated. The crude material was purified by flash chromatography on silica gel (eluent: hexane–EtOAc 90:10) to give (*rac*)-14 (7.0 g, 88%) as a colorless oil. TLC, R_f (*c*-hexane–EtOAc 90:10) = 0.25. MS (LC-MS): 324.2 [M + H]⁺. t_R (HPLC, Waters Symmetry C18, 3.5 μm , 2.1 mm × 50 mm, 20–95% CH_3CN – H_2O /3.5 min, 95% CH_3CN /2 min, CH_3CN and H_2O containing 0.1% TFA; flow, 0.6 mL/min): 2.7 min. ^1H NMR (DMSO- d_6 , 400 MHz): δ 1.08 (t, $J = 7.1$ Hz, 3H), 2.22 (dd, $J = 8.85$, 5.8 Hz, 1H), 2.55 (m, 1H), 2.66–2.70 (m, 5H), 2.76 (m, 1H), 3.47 (d, $J = 13.1$ Hz, 1H), 3.56 (d, $J = 13.1$ Hz, 1H), 3.95 (q, $J = 7.1$ Hz, 2H), 7.12–7.30 (m, 10H).

(3*S*,4*S**)-4-Benzylpyrrolidine-1,3-dicarboxylic Acid 1-*tert*-Butyl Ester 3-Ethyl Ester. A mixture of (*rac*)-14 (6.57 g, 20.3 mmol), di-*tert*-butylcarbonate (4.43 g, 20.3 mmol) and $\text{Pd}(\text{OH})_2$ (0.6 g, 50% wet) in EtOH (300 mL) was stirred under an hydrogen atmosphere for 20 h. After filtration through a pad of Celite, the filtrate was dried over Na_2SO_4 and concentrated. Purification of the residue by chromatography on silica gel (eluent: *c*-hexane–EtOAc 90:10) afforded (3*S*,4*S**)-4-benzylpyrrolidine-1,3-dicarboxylic acid 1-*tert*-butyl ester 3-ethyl ester (6.42 g, 95%). TLC, R_f (*c*-hexane–EtOAc 80:20) = 0.35. MS (LC-MS): 356.1 [M + Na]⁺. t_R (HPLC, Waters Symmetry C18, 3.5 μm , 2.1 mm × 50 mm, 20–95% CH_3CN – H_2O /3.5 min, 95% CH_3CN /2 min, CH_3CN and H_2O containing 0.1% TFA; flow, 0.6 mL/min): 4.1 min. ^1H NMR (DMSO- d_6 , 400 MHz): δ 1.14

(t, $J = 7.1$ Hz, 3H), 1.36 (s, 9H), 2.62 (m, 2H), 2.81 (m, 2H), 2.95 (m, 1H), 3.29–3.36 (m, 2H), 3.57 (m, 1H), 3.98 (q, $J = 7.1$ Hz, 2H), 7.19 (m, 3H), 7.27 (m, 2H).

(3*S*,4*S**)-3-Benzyl-4-hydroxymethyl-pyrrolidine-1-carboxylic Acid *tert*-Butyl Ester ((*rac*)-15). To a solution of (3*S*,4*S**)-4-benzylpyrrolidine-1,3-dicarboxylic acid 1-*tert*-butyl ester 3-ethyl ester (0.15 g, 0.45 mmol) in THF (4 mL) was slowly added a solution of LiBH_4 (2N in THF, 0.225 mL, 0.450 mmol) at 0 °C under an N_2 atmosphere. The reaction mixture was stirred overnight at RT, then refluxed for 2 h and subsequently carefully poured into an aqueous saturated NaHCO_3 solution. EtOAc was added, the layers were separated, and the aqueous phase was back-extracted twice with EtOAc. The combined organics were dried over Na_2SO_4 , filtered, and concentrated. The crude material was purified by flash chromatography on silica gel (eluent: *c*-hexane–EtOAc 100:0 to 80:20) to give (*rac*)-15 (0.79 g, 60%) as a colorless oil. TLC, R_f (*c*-hexane–EtOAc 80:20) = 0.20. MS (LC-MS): 236.1 [M-tBu + H]⁺. t_R (HPLC, Waters Symmetry C18, 3.5 μm , 2.1 mm × 50 mm, 20–95% CH_3CN – H_2O /3.5 min, 95% CH_3CN /2 min, CH_3CN and H_2O containing 0.1% TFA; flow, 0.6 mL/min): 3.4 min. ^1H NMR (DMSO- d_6 , 600 MHz): δ 1.35 (s, 9H), 1.96 (m, 1H), 2.14–2.24 (m, 1H), 2.46 (m, 1H), 2.81 (m, 1H), 2.90 (m, 1H), 3.05 (m, 1H), 3.20 (m, 1H), 3.30 (m, 1H), 3.37–3.45 (m, 2H), 4.65 (t, $J = 5.3$ Hz, 1H, OH), 7.18 (m, 3H), 7.27 (m, 2H). ^{13}C NMR (DMSO- d_6 , 150 MHz, 2 rotamers): δ 28.14, 37.73, 37.85, 40.35, 41.09, 44.76, 45.68, 48.33, 48.78, 50.61, 50.64, 61.29, 61.40, 78.08, 125.97, 128.28, 128.60, 140.24, 153.47, 153.50.

(3*S*,4*S**)-3-Benzyl-4-hydroxymethyl-pyrrolidine-1-carboxylic Acid *tert*-Butyl Ester (15a) and (3*R*,4*R**)-3-Benzyl-4-hydroxymethyl-pyrrolidine-1-carboxylic Acid *tert*-Butyl Ester (15b). (*Rac*)-15 (1.2 g) was separated into its enantiomers by preparative chiral HPLC column: Chiracel OJ, Diacel Chemical Industries Ltd., 10 cm × 50 cm, 20 μm ; eluent, hexane–EtOH 85:15; flow rate, 120 mL/min; detection, UV at 210 nm. (3*S*,4*S*)-15a: t_R 40.9 min (preparative chiral HPLC), t_R (HPLC, Chiracel OJ (1099), 0.46 cm × 25 cm, hexane/EtOH 90–10; flow, 1 mL/min): 7.1 min; enantiomeric excess $ee = 99.8\%$, $[\alpha]_D^{20} -48.4$ ($c = 0.99$, MeOH). The absolute configuration of the 2 stereogenic centers was determined based on X-ray structure crystallography of the corresponding (3*S*,4*R*)-3-benzyl-4-[(4-chlorophenylamino)-methyl]-pyrrolidine-1-carboxylic acid *tert*-butyl ester 17a^{26a} prepared in 2 steps as described below. (3*R*,4*R*)-15b: t_R 32.5 min (preparative chiral HPLC), t_R (HPLC, Chiracel OJ (1099), 0.46 cm × 25 cm, hexane–EtOH 90–10; flow, 1 mL/min): 5.2 min; enantiomeric excess $ee = 100\%$. $[\alpha]_D^{20} +46$ ($c = 1.02$, MeOH). The absolute configuration of the 2 stereogenic centers was determined based on X-ray structure crystallography of the corresponding (3*R*,4*S*)-3-benzyl-4-[(4-chlorophenylamino)-methyl]-pyrrolidine-1-carboxylic acid *tert*-butyl ester 17b^{26a} prepared in two steps as described below.

(3*S*,4*S**)-3-Benzyl-4-formyl-pyrrolidine-1-carboxylic Acid *tert*-Butyl Ester ((*rac*)-16). To a well stirred mixture of (*rac*)-15 (10.0 g, 34.3 mol) and Dess–Martin periodinane (14.6 g, 34.3 mmol) in CH_2Cl_2 (200 mL) was slowly added wet CH_2Cl_2 (0.68 mL of water in 50 mL of CH_2Cl_2 , 37.7 mmol). The clear solution turned cloudy toward the end of wet CH_2Cl_2 addition. The mixture was diluted with Et_2O and then concentrated by rotary evaporation to a small volume. The residue was taken up in Et_2O , washed with a 1:1 mixture of a 10% aqueous $\text{Na}_2\text{S}_2\text{O}_3$ solution and a saturated aqueous NaHCO_3 solution, followed by washing with H_2O and brine. The combined aqueous phases were back-extracted with Et_2O . The combined organics were washed with H_2O and brine, dried over Na_2SO_4 , filtered, and concentrated under reduced pressure. The crude material was purified by flash chromatography on silica gel (eluent: *c*-hexane–EtOAc 2:1) to give (*rac*)-16 as a slightly yellow oil (8.8 g, 89%). TLC, R_f (*c*-hexane–EtOAc 2:1) = 0.50. MS (LC-MS): 234.1 [M-tBu + H]⁺. t_R (HPLC, Waters Symmetry C18, 3.5 μm , 2.1 mm × 50 mm, 20–95% CH_3CN – H_2O /3.5 min, 95% CH_3CN /2 min, CH_3CN and H_2O containing 0.1% TFA; flow, 0.6 mL/min): 3.55 min. ^1H NMR (DMSO- d_6 , 600 MHz): δ 1.36 (s, 9H), 2.65–2.78 (m, 3H), 2.83 (m, 1H), 3.05 (m, 1H), 3.20 (m, 1H), 3.42 (m, 1H), 3.50 (m, 1H), 7.21 (m, 3H), 7.29 (m, 2H), 9.45 (m, 1H). ^{13}C NMR (DMSO- d_6 , 150 MHz, 2 rotamers): δ 28.1,

37.54, 39.99, 40.54, 44.43, 44.60, 49.91, 49.95, 53.64, 54.46, 78.55, 126.31, 128.82, 139.49, 153.35, 201.81, 201.87.

(3*S**,4*R**)-3-Benzyl-4-[(4-chlorophenylamino)-methyl]-pyrrolidine-1-carboxylic Acid *tert*-Butyl Ester ((*rac*)-17). A mixture of (*rac*)-16 (0.50 g, 1.72 mmol) and 4-chloroaniline (0.220 g, 1.69 mmol) in 1,2-dichloroethane (7 mL) was treated with sodium triacetoxyborohydride³⁹ (0.510 g, 2.42 mmol) with stirring at RT under a N₂ atmosphere overnight. The reaction was quenched by addition of aqueous saturated NaHCO₃ solution (10 mL), followed by extraction with CH₂Cl₂. The organic layer was dried over Na₂SO₄, filtered, and concentrated. The residual brown oil was purified by flash chromatography on silica gel (eluent: *c*-hexane–EtOAc 90:10) to give (*rac*)-17 (0.66 g, 95%). TLC, R_f (*c*-hexane–EtOAc 90:10) = 0.20. MS (LC–MS): 445.1 [M + HCOOH]⁺. t_R (HPLC, Waters Symmetry C18, 3.5 μm, 2.1 mm × 50 mm, 20–95% CH₃CN–H₂O/3.5 min, 95% CH₃CN/2 min, CH₃CN and H₂O containing 0.1% TFA; flow, 0.6 mL/min): 4.38 min. ¹H NMR (DMSO-*d*₆, 600 MHz): δ 1.35 (s, 9H), 2.10–2.15 (m, 1H), 2.20–2.28 (m, 1H), 2.52 (m, 1H), 2.84–2.97 (m, 3H), 3.02 (dd, *J* = 10.8, 7.6 Hz, 1H), 3.08 (m, 1H), 3.24 (m, 1H), 3.50 (m, 1H), 5.89 (m, 1H, NH), 6.51 (m, 2H), 7.05 (m, 2H), 7.19 (m, 3H), 7.28 (m, 2H). ¹³C NMR (DMSO-*d*₆, 150 MHz, 2 rotamers): δ 28.1, 37.69, 37.76, 41.67, 41.85, 42.59, 44.77, 44.84, 49.49, 49.94, 50.48, 50.56, 78.23, 113.18, 118.70, 126.03, 128.31, 128.52, 128.65, 140.13, 147.68, 153.45.

Crystallographic data (excluding structure factors) for (3*S*,4*R*)-17a and (3*R*,4*S*)-17b have been deposited with the Cambridge Crystallographic Data Centre as supplementary publication number CCDC 904172 (17a) and CCDC 904173 (17b). Copies of the data can be obtained, free of charge, on application to CCDC, 12 Union Road, Cambridge CB2 1EZ, UK [fax: +44-(0)1223–336033 or email: deposit@ccdc.cam.ac.uk].

(3*S*,4*R*)-3-Benzyl-4-[(4-chlorophenylamino)methyl]-pyrrolidine-1-carboxylic Acid *tert*-Butyl Ester ((3*S*,4*R*)-17a). The title compound was prepared as described for (*rac*)-17 from (3*S*,4*S*)-15a. [α]_D²⁰ = 33.1 (*c* = 1.17, MeOH). Absolute configuration determined by X-ray crystallography.^{26a}

(3*R*,4*S*)-3-Benzyl-4-[(4-chlorophenylamino)methyl]-pyrrolidine-1-carboxylic Acid *tert*-Butyl Ester ((3*R*,4*S*)-17b). The title compound was prepared as described for (*rac*)-17 from (3*R*,4*R*)-15b. [α]_D²⁰ = 33 (*c* = 0.96, MeOH). Absolute configuration determined by X-ray crystallography.^{26a}

(3*S**,4*R**)-3-Benzyl-4-(isopropylamino-methyl)-pyrrolidine-1-carboxylic Acid *tert*-Butyl Ester ((*rac*)-19). A mixture of (*rac*)-16 (2.64 g, 9.12 mmol), isopropylamine (2.35 mL, 27.4 mmol), and 1,2-dichloroethane (150 mL) was stirred at RT for 10 min. Sodium triacetoxyborohydride³⁹ (4.83 g, 22.8 mmol) was added, and the mixture was stirred for 20 h at RT. The reaction was quenched by addition of a saturated aqueous NaHCO₃ solution. After separation of the organic layer, the aqueous phase was extracted twice with CH₂Cl₂. The combined organics were dried over Na₂SO₄, and volatiles were removed in vacuo to afford (*rac*)-19 as a colorless oil (3.1 g, quantitative yield). t_R (HPLC, Waters Symmetry C18, 3.5 μm, 2.1 mm × 50 mm, 20–95% CH₃CN–H₂O/3.5 min, 95% CH₃CN/2 min, CH₃CN and H₂O containing 0.1% TFA; flow, 0.6 mL/min): 2.82 min. ¹H NMR (DMSO-*d*₆, 600 MHz): δ 0.94 (m, 6H), 1.35 (m, 9H), 1.94 (m, 1H), 2.11–2.19 (m, 1H), 2.39 (m, 1H), 2.45 (m, 1H), 2.64 (m, 2H), 2.82 (m, 1H), 2.89 (m, 1H), 2.98 (dd, *J* = 10.5, 7.9 Hz, 1H), 3.20 (m, 1H), 3.40 (m, 1H), 7.19 (m, 3H), 7.27 (m, 2H). ¹³C NMR (DMSO-*d*₆, 150 MHz, 2 rotamers): δ 21.28, 22.26, 22.50, 22.57, 28.16, 37.77, 37.84, 39.99, 42.00, 42.65, 42.73, 43.69, 48.37, 48.52, 49.99, 50.40, 50.58, 50.63, 78.12, 125.98, 128.28, 128.30, 128.64, 140.24, 153.44, 153.47, 172.17.

(3*S*,4*R*)-3-Benzyl-4-(isopropylamino-methyl)-pyrrolidine-1-carboxylic Acid *tert*-Butyl Ester ((3*S*,4*R*)-19a). The title compound was prepared as described for (*rac*)-19 in two steps from (3*S*,4*S*)-15a. [α]_D²⁰ = 44.9 (*c* = 1.18, MeOH).

(3*R*,4*S*)-3-Benzyl-4-(isopropylamino-methyl)-pyrrolidine-1-carboxylic Acid *tert*-Butyl Ester ((3*R*,4*S*)-19b). The title compound was prepared as described for (*rac*)-19 in two steps from (3*R*,4*R*)-15b. [α]_D²⁰ = 40.9 (*c* = 1.16, MeOH).

Preparation of Compounds 6(a,b), (*rac*) 7–11, 12(a,b), ((3*S*,4*S*)-4-Benzylpyrrolidin-3-ylmethyl)-(4-chlorophenyl)-phenylamine Hydrochloride Salt (6a) and ((3*R*,4*R*)-4-Benzylpyrrolidin-3-ylmethyl)-(4-chlorophenyl)-phenylamine Hydrochloride Salt (6b), ((3*S,4*S**)-4-Benzylpyrrolidin-3-ylmethyl)-(4-chlorophenyl)-phenylamine, (*rac*)-6,⁴⁰ (215 mg) was separated into its enantiomers by preparative chiral HPLC column: Chiracel OD prep, Daicel Chemical Industries Ltd., 50 mm × 500 mm (20 μm); eluent, hexane–EtOH 95:5 + 0.1% TFA; flow rate, 80 mL/min; detection, UV at 210 nm. (3*S*,4*S*)-6a: The product (contaminated with residual trifluoroacetic acid) was isolated as peak 1 with t_R 52.7 min (preparative chiral HPLC). This material was dissolved in CH₂Cl₂ and subsequently washed with a saturated aqueous solution of NaHCO₃. The organics were dried over Na₂SO₄, filtered, and concentrated. The residue was dissolved in dioxane (1 mL), followed by addition of 4 M HCl in dioxane (1 equiv) and lyophilization to afford (3*S*,4*S*)-6a, HCl salt, (67 mg). ¹H NMR (DMSO-*d*₆, 600 MHz): δ 2.25 (m, 1H), 2.31 (m, 1H), 2.65 (dd, *J* = 13.5, 8.3 Hz, 1H), 2.75 (dd, *J* = 13.5, 6.6 Hz, 1H), 2.83 (m, 1H), 2.91 (m, 1H), 3.18 (m, 1H), 3.26 (m, 1H), 3.64 (dd, *J* = 14.8, 5.6 Hz, 1H), 3.72 (dd, *J* = 14.8, 9.2 Hz, 1H), 6.79 (d, *J* = 8.9 Hz, 2H), 6.95 (d, *J* = 7.9 Hz, 2H), 7.04 (t, *J* = 7.6 Hz, 1H), 7.14 (d, *J* = 7.25 Hz, 2H), 7.23 (m, 3H), 7.30 (m, 4H), 9.03 (m, 1H), 9.1 (m, 1H). ¹³C NMR (DMSO-*d*₆, 150 MHz): δ 37.43, 41.12, 42.22, 48.14, 49.16, 53.37, 120.95, 122.66, 122.96, 124.31, 126.40, 128.51, 128.78, 129.02, 129.64, 139.33, 146.81, 146.99. t_R (HPLC, Waters Symmetry C18, 3.5 μm, 2.1 mm × 50 mm, 20–95% CH₃CN–H₂O/3.5 min, 95% CH₃CN/2 min, CH₃CN and H₂O containing 0.1% TFA; flow, 0.6 mL/min): 3.46 min, purity 99.3%. t_R (Waters XBridge C18, 2.5 μm, 3 mm × 50 mm, 10–98% CH₃CN–H₂O/8.6 min, 98% CH₃CN/1.4 min, CH₃CN and H₂O containing 0.1% TFA; flow, 1.4 mL/min, temperature 40 °C): 4.69 min, purity 99%. t_R (HPLC, Daicel OD-H, 250 mm × 4.6 mm (5 μm), hexane–EtOH 95:5 + 0.1% TFA, flow 1 mL/min, UV 210 nm, injection volume 10 μL of a 0.1% solution in EtOH): 14.5 min; enantiomeric excess *ee* > 99.9%. HRMS calcd for C₂₄H₂₅ClN₂ [M + H]⁺, 377.1779; found, 377.1778. (3*R*,4*R*)-6b: The product (contaminated with residual trifluoroacetic acid) was isolated as peak 2 with t_R 76.4 min (preparative chiral HPLC). This material was dissolved in CH₂Cl₂ and subsequently washed with a saturated aqueous solution of NaHCO₃. The organics were dried over Na₂SO₄, filtered, and concentrated. The residue was dissolved in dioxane (1 mL), followed by addition of 4 M HCl in dioxane (1 equiv) and lyophilization to afford (3*R*,4*R*)-6b, HCl salt, (80 mg). t_R (HPLC, Waters Symmetry C18, 3.5 μm, 2.1 mm × 50 mm, 20–95% CH₃CN–H₂O/3.5 min, 95% CH₃CN/2 min, CH₃CN and H₂O containing 0.1% TFA; flow, 0.6 mL/min): 3.44 min, purity 100%. t_R (Waters XBridge C18, 2.5 μm, 3 mm × 50 mm, 10–98% CH₃CN–H₂O/8.6 min, 98% CH₃CN/1.4 min, CH₃CN and H₂O containing 0.1% TFA; flow, 1.4 mL/min, temperature 40 °C): 4.70 min, purity 99%. t_R (HPLC, Daicel OD-H, 250 mm × 4.6 mm (5 μm), hexane–EtOH 95:5 + 0.1% TFA, flow 1 mL/min, UV 210 nm, injection volume 10 μL of a 0.1% solution in EtOH): 18.7 min; enantiomeric excess *ee* > 99.9%. HRMS calcd for C₂₄H₂₅ClN₂ [M + H]⁺, 377.1779; found, 377.1779.**

The synthesis of (3*S*,4*S*)-6a, HCl salt, was also accomplished in two steps starting from enantiomerically pure (3*S*,4*R*)-17a of known absolute configuration (vide infra) according to the following procedure:

(3*S*,4*R*)-3-Benzyl-4-[(4-chlorophenyl)-phenylamino]-methyl]-pyrrolidine-1-carboxylic Acid *tert*-Butyl Ester. A dry three-necked flask equipped with a magnetic stirring bar, septum, and condenser with an argon inlet–outlet was charged with [Pd(μ-Br)(*t*-Bu₃P)]₂⁴¹ (9.70 mg, 0.0125 mmol), sodium *tert*-butoxide (35.5 mg, 0.37 mmol), bromobenzene (59 mg, 0.37 mmol), and dry toluene (0.5 mL). A solution of (3*S*,4*R*)-17a (100 mg, 0.25 mmol) in dry degassed toluene (1 mL) was added, and the mixture was stirred at RT for 15 min, followed by heating to 110 °C (gentle reflux) overnight. After cooling to RT, the mixture was poured into water and the water phase was extracted twice with EtOAc. The combined organic extracts were dried over Na₂SO₄, filtered, and concentrated. The crude product was purified by flash chromatography on silica gel (eluent: *c*-hexane–EtOAc 90:10) to afford the title compound (91 mg, 76%). TLC, R_f (*c*-

hexane–EtOAc 80:20) = 0.50. MS (LC–MS): 421 [M+H]⁺, 477 [M+H]⁺, 499 [M+Na]⁺. *t*_R (HPLC, Waters Symmetry C18, 3.5 μm, 2.1 mm × 50 mm, 20–95% CH₃CN–H₂O/3.5 min, 95% CH₃CN/2 min, CH₃CN and H₂O containing 0.1% TFA; flow, 0.6 mL/min): 5.16 min. ¹H NMR (CDCl₃, 400 MHz): δ 1.43 (s, 9H), 2.25 (m, 1H), 2.33 (m, 1H), 2.60 (m, 1H), 2.78 (m, 1H), 3.04–3.21 (m, 2H), 3.43 (m, 1H), 3.53 (dd, *J* = 14.6, 8.85 Hz, 1H), 3.59 (m, 1H), 3.73 (m, 1H), 6.76 (d, *J* = 8.4 Hz, 2H), 6.91 (d, *J* = 7.8 Hz, 2H), 7.0 (t, *J* = 7.3 Hz, 1H), 7.09 (m, 2H), 7.16 (m, 2H), 7.24–7.28 (m, 5H).

((3*S*,4*S*)-4-Benzyl-pyrrolidin-3-ylmethyl)-(4-chlorophenyl)-phenylamine, (3*S*,4*S*)-6a, Hydrochloride Salt. To a solution of (3*S*,4*R*)-3-benzyl-4-[(4-chlorophenyl)-phenylamino]-methyl-pyrrolidine-1-carboxylic acid *tert*-butyl ester (91 mg, 0.19 mmol) in dioxane (2 mL) was added 1 M HCl in dioxane (2 mL), and the reaction mixture was stirred at RT for 4 h followed by lyophilization to afford (3*S*,4*S*)-6a, HCl salt (78 mg, quantitative yield). The product thus obtained showed the same retention time as the corresponding enantiomer (peak 1, vide supra) by analytical chiral HPLC. *t*_R (HPLC, Daicel OD-H, 250 mm × 4.6 mm (5 μm), hexane–EtOH 95:5 + 0.1% TFA, flow 1 mL/min, UV 210 nm, injection volume 10 μL of a 0.1% solution in EtOH): 14.5 min.

Preparation of (rac)-7, HCl Salt. (3*S**,4*R**)-3-Benzyl-4-[(benzyl-(4-chlorophenyl)-amino)-methyl]-pyrrolidine-1-carboxylic Acid *tert*-Butyl Ester. To a solution of (rac)-17 (80 mg, 0.20 mmol) in DMF (1 mL) were added K₂CO₃ (0.062 g, 0.44 mmol) and benzylbromide (0.052 mL, 0.44 mmol). Stirring was continued at 80 °C for 5 h before the reaction mixture was quenched with a saturated aqueous NaHCO₃ solution. The water phase was extracted with EtOAc, and the combined organics were dried over Na₂SO₄, filtered, and concentrated. The crude residue was purified by flash chromatography (eluent: *c*-hexane–EtOAc 95:5 to 90:10) to give the title compound (64 mg, 65%). TLC, *R*_f (*c*-hexane–EtOAc 80:20) = 0.55. ¹H NMR (CD₃OD, 400 MHz): δ 1.39 (s, 9H), 2.18 (m, 1H), 2.32 (m, 1H), 2.50 (m, 1H), 2.73 (dd, *J* = 17.9, 8.9 Hz, 1H), 3.0 (dd, *J* = 14.8, 8.6 Hz, 1H), 3.23–3.06 (m, 2H), 3.34–3.49 (m, 3H), 4.42 (m, 2H), 6.55 (d, *J* = 12.1 Hz, 2H), 6.99–7.31 (m, 12H).

Benzyl-((3*S,4*S**)-4-benzylpyrrolidin-3-ylmethyl)-(4-chlorophenyl)-amine (rac)-7, Hydrochloride Salt.** To a solution of (3*S**,4*R**)-3-benzyl-4-[(benzyl-(4-chlorophenyl)-amino)-methyl]-pyrrolidine-1-carboxylic acid *tert*-butyl ester (64 mg, 0.13 mmol) in CH₂Cl₂ (2 mL) was added trifluoroacetic acid (0.05 mL), and the mixture was stirred at RT overnight. Volatile were removed under reduced pressure. The mixture was then poured into a saturated aqueous solution of NaHCO₃, the water phase was extracted with EtOAc, and the combined organics were dried over Na₂SO₄ and concentrated. The crude residue was purified by Isolute Flash NH₂ ion exchange chromatography (eluent: CH₂Cl₂–MeOH 97:3 to 90:10 + 1% of NH₄OH) to give (rac)-7 as the free base (44.2 mg, 87%). This material was dissolved in dioxane (2 mL), followed by addition of 4 M HCl in dioxane (28 μL, 0.113 mmol) and lyophilization to afford (rac)-7, HCl salt (94% purity by HPLC using two analytical methods). MS (LC–MS): 391, 393 [M+H]⁺. *t*_R (Waters XBridge C18, 2.5 μm, 3 mm × 30 mm, 10–98% CH₃CN/H₂O/3 min, 98% CH₃CN/0.5 min, CH₃CN and H₂O containing 0.1% TFA; flow, 1.4 mL/min; temperature 40 °C): 2.34 min, purity 99%. *t*_R (Waters XBridge C18, 2.5 μm, 3 mm × 50 mm, 10–98% CH₃CN–H₂O/8.6 min, 98% CH₃CN/1.4 min, CH₃CN and H₂O containing 0.1% TFA; flow, 1.4 mL/min; temperature 40 °C): 4.73 min, purity 99%. ¹H NMR (DMSO-*d*₆, 600 MHz): δ 2.31 (m, 1H), 2.41 (m, 1H), 2.68 (m, 1H), 2.78 (m, 1H), 2.86 (m, 1H), 3.02 (m, 1H), 3.23 (m, 1H), 3.30 (m, 1H), 3.42–3.49 (m, 2H), 4.55 (bs, 2H), 6.50 (d, *J* = 8.95 Hz, 2H), 7.05 (d, *J* = 8.95 Hz, 2H), 7.08 (d, *J* = 7.3 Hz, 2H), 7.18–7.24 (m, 4H), 7.28–7.32 (m, 4H), 9.05 (m, 1H), 9.12 (m, 1H). ¹³C NMR (DMSO-*d*₆, 150 MHz): δ 37.78, 40.71, 42.17, 47.86, 49.21, 53.09, 54.15, 114.01, 119.77, 126.38, 126.69, 128.48, 128.52, 128.59, 128.80, 138.23, 139.49, 146.37. HRMS calcd for C₂₃H₂₈ClN₂ [M+H]⁺, 391.1936; found, 391.1933.

Preparation of (rac)-8, HCl Salt. (3*S**,4*R**)-3-Benzyl-4-[(4-chlorophenyl)-[4-methoxy-3-(3-methoxypropoxy)-benzyl]-amino]-methyl-pyrrolidine-1-carboxylic Acid *tert*-Butyl Ester. The title

compound was prepared using the same procedure as described for (rac)-7 using 4-bromomethyl-1-methoxy-2-(3-methoxypropoxy)-benzene⁴⁰ for the alkylation reaction. The crude product obtained after aqueous workup was purified by preparative HPLC (Waters Sunfire C18-OBD, 5 μm, 19 mm × 50 mm; eluent, 20% CH₃CN/1 min, 20–100% CH₃CN–H₂O/16 min, 100% CH₃CN/4 min, CH₃CN and H₂O containing 0.1% HCOOH; flow, 20 mL/min). The HPLC fractions were collected, concentrated, diluted with EtOAc, and washed with a saturated aqueous solution of NaHCO₃. The organic layer was dried over Na₂SO₄, filtered, and concentrated to give the title compound (73 mg, 48%). TLC, *R*_f (CH₂Cl₂–MeOH 95:5) = 0.45. MS (LC–MS): 609.2 [M+H]⁺. *t*_R (HPLC, Waters Symmetry C18, 3.5 μm, 2.1 mm × 50 mm, 5–95% CH₃CN–H₂O/3.5 min, 95% CH₃CN/2 min, CH₃CN and H₂O containing 0.1% TFA; flow, 0.6 mL/min): 4.7 min. ¹H NMR (DMSO-*d*₆, 400 MHz): δ 1.33 (s, 9H), 1.87 (p, *J* = 6.4 Hz, 2H), 2.20–2.31 (m, 2H), 2.45–2.53 (m, 1H), 2.80 (dd, *J* = 13.6, 5.3 Hz, 1H), 2.94 (m, 1H), 3.05 (m, 1H), 3.20 (s, 3H), 3.25 (m, 1H), 3.30–3.35 (m, 1H), 3.41 (t, *J* = 6.4 Hz, 2H), 3.41–3.46 (m, 1H), 3.48 (m, 1H), 3.68 (s, 3H), 3.89 (t, *J* = 6.4 Hz, 2H), 4.44 (m, 2H), 6.60 (m, 1H), 6.63 (d, *J* = 8.8 Hz, 2H), 6.73 (m, 1H), 6.84 (d, *J* = 8.1 Hz, 1H), 7.08 (d, *J* = 8.8 Hz, 2H), 7.16 (m, 3H), 7.26 (m, 2H). ¹³C NMR (DMSO-*d*₆, 150 MHz, 2 rotamers): δ 28.09, 28.94, 37.82, 37.94, 40.96, 41.61, 41.98, 42.72, 49.26, 50.30, 50.40, 53.04, 53.24, 54.00, 54.06, 55.51, 57.91, 65.22, 68.47, 69.76, 78.19, 78.25, 111.80, 112.04, 114.25, 114.31, 118.59, 118.64, 119.61, 126.04, 128.31, 128.50, 128.60, 128.63, 130.52, 140.10, 146.96, 147.03, 147.81, 147.98, 153.40.

N-((3*S,4*S**)-4-Benzylpyrrolidin-3-yl-methyl)-(4-chlorophenyl)-[4-methoxy-3-(3-methoxypropoxy)-benzyl]-amine (rac)-8, Hydrochloride Salt.** To a solution of (3*S**,4*R**)-3-benzyl-4-[(4-chlorophenyl)-[4-methoxy-3-(3-methoxypropoxy)-benzyl]-amino]-methyl-pyrrolidine-1-carboxylic acid *tert*-butyl ester (52 mg, 0.085 mmol) in dioxane (2 mL) was added 4 M HCl in dioxane (1 mL) followed by stirring for 2 h at RT. Lyophilization afforded (rac)-8, HCl salt, as a solid (50 mg, 100%). MS (LC–MS): 509.1 [MH]⁺. *t*_R (Waters XBridge C18, 2.5 μm, 3 mm × 30 mm, 10–98% CH₃CN/H₂O/3 min, 98% CH₃CN/0.5 min, CH₃CN and H₂O containing 0.1% TFA; flow, 1.4 mL/min; temperature 40 °C): 2.18 min, purity 99%. *t*_R (Waters XBridge C18, 2.5 μm, 3 mm × 50 mm, 10–98% CH₃CN–H₂O/8.6 min, 98% CH₃CN/1.4 min, CH₃CN and H₂O containing 0.1% TFA; flow, 1.4 mL/min, temperature 40 °C): 4.58 min, purity 99%. ¹H NMR (DMSO-*d*₆, 600 MHz): δ 1.87 (p, *J* = 6.3 Hz, 2H), 2.31 (m, 1H), 2.38 (m, 1H), 2.66 (dd, *J* = 13.5, 8.2 Hz, 1H), 2.76 (dd, *J* = 13.5, 7.0 Hz, 1H), 2.86 (m, 1H), 3.0 (m, 1H), 3.21 (s, 3H), 3.22 (m, 1H), 3.28 (m, 1H), 3.38 (m, 2H), 3.41 (t, *J* = 6.3 Hz, 2H), 3.68 (s, 3H), 3.89 (m, 2H), 4.44 (d, *J* = 16.8 Hz, 1H), 4.48 (d, *J* = 16.8 Hz, 1H), 6.53 (d, *J* = 8.9 Hz, 2H), 6.55 (m, 1H), 6.71 (m, 1H), 6.82 (d, *J* = 8.2 Hz, 1H), 7.06 (d, *J* = 8.9 Hz, 2H), 7.19–7.23 (m, 3H), 7.31 (m, 2H), 8.98 (m, 1H), 9.05 (m, 1H). ¹³C NMR (DMSO-*d*₆, 150 MHz): δ 28.95, 37.74, 40.70, 42.20, 47.96, 49.23, 52.98, 54.05, 55.52, 57.93, 65.25, 68.46, 111.77, 112.05, 114.29, 118.51, 119.84, 126.38, 128.51, 128.54, 128.78, 130.39, 139.49, 146.53, 147.84, 147.99. HRMS calcd for C₃₀H₃₈ClN₂O₃ [M+H]⁺, 509.2566; found, 509.2563. HRMS calcd for C₃₀H₃₇ClN₂O₃Na [M+Na]⁺, 531.2385; found, 531.2385.

Preparation of (rac)-9, HCl Salt. (3*S**,4*R**)-3-Benzyl-4-[(*iso*-propyl-[4-methoxy-3-(3-methoxypropoxy)-benzyl]-amino)-methyl]-pyrrolidine-1-carboxylic Acid *tert*-Butyl Ester. A mixture of (rac)-19 (300 mg, 0.9 mmol) and 4-methoxy-3-(3-methoxypropoxy)-benzaldehyde⁴⁰ (202 mg, 0.90 mmol) in 1,2-dichloroethane (5 mL) was treated with sodium triacetoxyborohydride³⁹ (765 mg, 3.61 mmol) with stirring at RT under a N₂ atmosphere overnight and was then poured into an aqueous saturated solution of NaHCO₃. The layers were separated, and the water phase was extracted twice with CH₂Cl₂. The combined organics were dried over Na₂SO₄, filtered, and concentrated. The residue was purified by preparative HPLC (YMC-Pack C18-ODS-AQ 5 μm, 20 mm × 50 mm; eluent, 5% CH₃CN/2.5 min, 5–100% CH₃CN–H₂O/10.5 min, 100% CH₃CN/5 min, CH₃CN and H₂O containing 0.1% HCOOH; flow, 20 mL/min). The compound containing HPLC fractions were collected, diluted with EtOAc, and washed with a saturated aqueous solution of NaHCO₃. The organic layer was dried over Na₂SO₄, filtered, and concentrated to give the title

compound (72 mg, 15%). MS (LC–MS): 541 [M + H]⁺. ¹H NMR (DMSO-*d*₆, 400 MHz): δ 0.90 (m, 6H), 1.32 (m, 9H), 1.89 (m, 2H), 1.99 (m, 1H), 2.08–2.22 (m, 2H), 2.31 (m, 1H), 2.44 (m, 1H), 2.75 (m, 2H), 2.85–2.94 (m, 2H), 3.08 (m, 1H), 3.20 (s, 3H), 3.35 (m, 2H), 3.39 (m, 1H), 3.42 (t, *J* = 6.1 Hz, 2H), 3.70 (s, 3H), 3.93 (m, 2H), 6.75 (m, 1H), 6.85 (m, 2H), 7.15 (m, 3H), 7.26 (m, 2H).

(3S*,4S*)-4-Benzylpyrrolidin-3-ylmethyl-isopropyl-[4-methoxy-3-(3-methoxypropoxy)benzyl]-amine, (rac)-9, Hydrochloride Salt. To a solution of (3S*,4R*)-3-benzyl-4-({isopropyl-[4-methoxy-3-(3-methoxypropoxy)-benzyl]-amino}-methyl)-pyrrolidine-1-carboxylic acid *tert*-butyl ester (72.0 mg, 0.133 mmol) in CH₂Cl₂ (2 mL) was added trifluoroacetic acid (0.1 mL), and the mixture was stirred at RT for 1 h. The mixture was then poured into a saturated aqueous solution of NaHCO₃, extracted with EtOAc, dried over Na₂SO₄, and concentrated. The crude residue was purified by Isolute Flash NH₂ ion exchange chromatography (eluent: CH₂Cl₂–MeOH 100:0 to 90:10 + 5% of NH₄OH) to give (rac)-9 as the free base (47.7 mg). This material was dissolved in dioxane (2 mL), followed by addition of 4 M HCl in dioxane (27 μL, 0.11 mmol) and lyophilization to afford (rac)-9, HCl salt (48 mg, 86%). MS (LC–MS): 441 [M + H]⁺. *t*_R (HPLC, Waters Symmetry C18, 3.5 μm, 2.1 mm × 50 mm, 20–95% CH₃CN–H₂O/3.5 min, 95% CH₃CN/2 min, CH₃CN and H₂O containing 0.1% TFA; flow, 0.6 mL/min): 2.18 min; purity 100%. *t*_R (HPLC, MN Nucleosil C18HD, 3 μm, 70 mm × 4 mm, 20–95% CH₃CN–H₂O/3.5 min, 95% CH₃CN/2 min, CH₃CN and H₂O containing 0.1% TFA; flow, 0.6 mL/min): 3.57 min; purity 100%. ¹H NMR (DMSO-*d*₆, 400 MHz, 394 K): δ 1.12 (m, 6H), 1.94 (m, 2H), 2.25 (m, 2H), 2.52 (m, 1H), 2.80–2.90 (m, 2H), 3.12 (dd, *J* = 17.0, 10.6 Hz, 1H), 3.25 (s, 3H), 3.25 (m, 1H), 3.46 (m, 1H), 3.48 (t, *J* = 9.5 Hz, 2H), 3.51 (m, 1H), 3.77 (s, 3H), 3.78 (m, 2H), 4.04 (m, 2H), 6.90 (m, 1H), 6.94–7.10 (m, 2H), 7.19 (m, 3H), 7.27 (m, 2H), 9.19 (m, 2H). HRMS calcd for C₂₇H₄₁N₂O₃ [M + H]⁺, 441.3112; found, 441.3110.

Preparation of (rac)-10, HCl Salt. *N*-((3S*,4S*)-4-Benzylpyrrolidin-3-ylmethyl)-*N*-(4-chlorophenyl)-4-methoxy-3-(3-methoxypropoxy)benzamide, (rac)-10. The title compound was prepared as described for (rac)-12 in two steps from (rac)-17. MS (LC–MS): 523.4 [M + H]⁺. *t*_R (HPLC, Waters Symmetry C18, 3.5 μm, 2.1 mm × 50 mm, 20–95% CH₃CN/H₂O/3.5 min, 95% CH₃CN/2 min, CH₃CN and H₂O containing 0.1% TFA; flow, 0.6 mL/min): 3.01 min; purity 97%. *t*_R (Waters XBridge C18, 2.5 μm, 3 mm × 50 mm, 10–98% CH₃CN–H₂O/8.6 min, 98% CH₃CN/1.4 min, CH₃CN and H₂O containing 0.1% TFA; flow, 1.4 mL/min, temperature 40 °C): 3.96 min, purity 96%. ¹H NMR (DMSO-*d*₆, 600 MHz): δ 1.78 (m, 2H), 2.09 (m, 1H), 2.32 (m, 1H), 2.59 (dd, *J* = 13.3, 7.9 Hz, 1H), 2.69 (dd, *J* = 13.3, 6.6 Hz, 1H), 2.85 (m, 1H), 3.0 (m, 1H), 3.22 (m, 1H), 3.23 (s, 3H), 3.30–3.39 (m, 3H), 3.69 (s, 3H), 3.73 (m, 2H), 3.90 (bd, *J* = 7.0 Hz, 2H), 6.72 (m, 1H), 6.80 (m, 2H), 7.0 (d, *J* = 8.4 Hz, 2H), 7.10 (d, *J* = 7.3 Hz, 2H), 7.21 (m, 1H), 7.25 (m, 2H), 7.30 (d, *J* = 8.4 Hz, 2H), 8.91 (m, 2H). ¹³C NMR (DMSO-*d*₆, 150 MHz): δ 28.68, 36.73, 39.98, 41.03, 42.11, 48.05, 48.87, 50.26, 55.41, 57.95, 65.23, 68.34, 110.71, 113.57, 122.22, 126.38, 127.33, 128.47, 128.86, 129.16, 129.36, 130.94, 139.11, 141.80, 146.60, 150.12, 169.30. HRMS calcd for C₃₀H₃₆ClN₂O₄ [M + H]⁺, 523.2358; found, 523.2358.

Preparation of (rac)-11, HCl Salt. *N*-((3S*,4S*)-4-Benzylpyrrolidin-3-ylmethyl)-*N*-phenyl-4-methoxy-3-(3-methoxypropoxy)-benzamide, (rac)-11, Hydrochloride Salt. The title compound was prepared as described for (rac)-12 in two steps from (rac)-18 (prepared as described for (rac)-17 using aniline instead of 4-chloroaniline). MS (LC–MS): 489 [M + H]⁺. *t*_R (Waters XBridge C18, 2.5 μm, 3 mm × 30 mm, 10–98% CH₃CN/H₂O/3 min, 98% CH₃CN/0.5 min, CH₃CN and H₂O containing 0.1% TFA; flow, 1.4 mL/min, temperature 40 °C): 1.81 min, purity 100%. *t*_R (Waters XBridge C18, 2.5 μm, 3 mm × 50 mm, 10–98% CH₃CN–H₂O/8.6 min, 98% CH₃CN/1.4 min, CH₃CN and H₂O containing 0.1% TFA; flow, 1.4 mL/min; temperature 40 °C): 3.57 min, purity 100%. ¹H NMR (DMSO-*d*₆, 600 MHz): δ 1.77 (m, 2H), 2.12 (m, 1H), 2.34 (m, 1H), 2.60 (dd, *J* = 13.55, 8.1 Hz, 1H), 2.70 (dd, *J* = 13.55, 6.6 Hz, 1H), 2.84 (dd, *J* = 11.5, 7.6 Hz, 1H), 3.0 (dd, *J* = 11.9, 7.6 Hz, 1H), 3.21 (dd, *J* = 11.5, 7.4 Hz, 1H), 3.23 (s, 3H), 3.37 (t, *J* = 6.2 Hz, 3H), 3.68

(m, 5H), 3.90 (dd, *J* = 14.0, 8.2 Hz, 1H), 3.96 (dd, *J* = 14.0, 6.1 Hz, 1H), 6.69 (d, *J* = 2.0 Hz, 1H), 6.76 (d, *J* = 8.4 Hz, 1H), 6.82 (dd, *J* = 8.4, 2.0 Hz, 1H), 6.99 (d, *J* = 7.4 Hz, 2H), 7.11 (m, 2H), 7.17–7.22 (m, 2H), 7.25 (m, 4H), 8.94 (m, 2H). ¹³C NMR (DMSO-*d*₆, 150 MHz): δ 28.7, 36.77, 41.20, 42.19, 48.07, 48.82, 50.40, 55.38, 57.39, 65.16, 68.35, 110.62, 113.53, 122.19, 126.34, 126.62, 127.61, 128.47, 128.86, 128.94, 129.24, 139.14, 142.91, 146.49, 149.96, 169.31. HRMS: 489.27470 [M + H]⁺ (calcd 489.27478 for C₃₀H₃₆N₂O₄).

Preparation of (rac)-12, (3S,4S)-12a, (3R,4R)-12b, HCl Salt. (3S*,4R*)-3-Benzyl-3-({isopropyl-[4-methoxy-3-(3-methoxypropoxy)-benzoyl]-amino}-methyl)-pyrrolidine-1-carboxylic Acid *tert*-Butyl Ester. A mixture of (rac)-19 (600 mg, 1.80 mmol), 4-methoxy-3-(3-methoxypropoxy)-benzoyl chloride⁴⁰ (512 mg, 1.98 mmol), and triethylamine (326 μL, 2.34 mmol) in CH₂Cl₂ (6 mL) was stirred at RT overnight and then quenched by the addition of an aqueous NaHCO₃ solution. The organic layer was separated, and the aqueous phase was extracted three times with CH₂Cl₂. The combined organic extracts were dried (Na₂SO₄), and volatiles were removed in vacuo. The crude product was purified by flash chromatography (eluent: *c*-hexane–EtOAc 2:1) to afford the title compound (791 mg, 79%). MS (LC–MS): 455 [M–Boc + H]⁺. ¹H NMR (MeOD, 400 MHz): δ 1.12 (m, 6H), 1.45 (s, 9H), 2.03 (m, 2H), 2.32–2.43 (m, 2H), 2.62 (m, 1H), 2.84 (m, 1H), 3.09 (m, 1H), 3.23 (m, 2H), 3.25 (s, 3H), 3.46–3.56 (m, 3H), 3.57 (m, 2H), 3.86 (s, 3H), 4.07 (m, 3H), 6.90 (m, 2H), 7.19 (m, 4H), 7.27 (m, 2H).

N-((3S*,4S*)-4-Benzylpyrrolidin-3-ylmethyl)-*N*-isopropyl-4-methoxy-3-(3-methoxypropoxy)benzamide, (rac)-12, Hydrochloride Salt. To a solution of (3S*,4R*)-3-benzyl-4-({isopropyl-[4-methoxy-3-(3-methoxypropoxy)-benzoyl]-amino}-methyl)-pyrrolidine-1-carboxylic acid *tert*-butyl ester (343.4 mg, 0.619 mmol) in 2-propanol (2 mL) was added 6 M HCl in 2-propanol (1 mL), and stirring was continued for 2 h at RT. The reaction mixture was concentrated, diluted with CH₂Cl₂, and neutralized by the addition of 1 N NaOH. The aqueous phase was extracted three times with CH₂Cl₂, and the combined organics were dried over Na₂SO₄, filtered, and concentrated. The crude residue was purified by preparative HPLC (Macherey-Nagel C18 Nucleosil-100 10 μm, 40 mm × 250 mm; eluent, 20–100% CH₃CN/10 min, 100% CH₃CN/10 min, CH₃CN and H₂O containing 0.1% TFA; flow, 40 mL/min). The compound containing fractions were combined and concentrated in vacuo. The residue was diluted with CH₂Cl₂, neutralized by addition of a saturated aqueous solution of NaHCO₃, and extracted three times with CH₂Cl₂. The combined organic extracts were dried over Na₂SO₄, filtered, and concentrated to afford (rac)-12 as the free base (214 mg, 76%). ¹H NMR (DMSO-*d*₆, 400 MHz, 394 K): δ 1.07 (d, *J* = 6.7 Hz, 3H), 1.11 (d, *J* = 6.7 Hz, 3H), 1.93 (p, *J* = 6.3 Hz, 2H), 2.10–2.22 (m, 2H), 2.59 (m, 2H), 2.78 (m, 1H), 2.97 (dd, *J* = 8.0, 7.5 Hz, 1H), 3.09 (dd, *J* = 11.2, 7.5 Hz, 1H), 3.25 (s, 3H), 3.26 (m, 2H), 3.48 (t, *J* = 6.3 Hz, 2H), 3.80 (s, 3H), 3.96 (m, 1H), 4.02 (t, *J* = 6.3 Hz, 2H), 6.86 (m, 2H), 6.96 (m, 1H), 7.18 (m, 3H), 7.27 (m, 2H).

To a solution of (rac)-12, free base, in dioxane was added 4N HCl in dioxane (117 μL, 0.470 mmol) followed by lyophilization to afford the (rac)-12, HCl salt. MS (LC–MS): 455 [M + H]⁺. *t*_R (HPLC, Waters Symmetry C18, 3.5 μm, 2.1 mm × 50 mm, 20–95% CH₃CN–H₂O/3.5 min, 95% CH₃CN/2 min, CH₃CN and H₂O containing 0.1% TFA; flow, 0.6 mL/min): 2.75 min, purity 96%. *t*_R (HPLC, MN Nucleosil C18HD, 3 μm, 70 mm × 4 mm, 20–95% CH₃CN–H₂O/3.5 min, 95% CH₃CN/2 min, CH₃CN and H₂O containing 0.1% TFA; flow, 0.6 mL/min): 4.15 min, purity 96.5%. ¹H NMR (DMSO-*d*₆, 600 MHz): δ 0.96 (m, 3H), 1.04 (m, 3H), 1.92 (m, 2H), 2.34 (m, 2H), 2.64 (m, 1H), 2.88 (m, 2H), 3.04 (m, 1H), 3.16 (m, 1H), 3.22 (s, 3H), 3.32 (m, 2H), 3.37 (m, 1H), 3.44 (m, 2H), 3.77 (s, 3H), 3.90 (m, 1H), 3.98 (m, 2H), 6.86 (m, 2H), 6.98 (m, 1H), 7.22 (m, 1H), 7.25 (m, 2H), 7.31 (m, 2H), 8.95 (m, 2H). HRMS calcd for C₂₇H₃₉N₂O₄, 455.2904 [M + H]⁺; found, 455.2904.

N-((3S,4S)-4-Benzylpyrrolidin-3-ylmethyl)-*N*-isopropyl-4-methoxy-3-(3-methoxypropoxy)benzamide, (3S,4S)-12a. The title compound was prepared in two steps as described for (rac)-12 from (3S,4R)-19a. *t*_R (Waters XBridge C18, 2.5 μm, 3 mm × 30 mm, 10–98% CH₃CN/H₂O/3 min, 98% CH₃CN/0.5 min, CH₃CN and H₂O

containing 0.1% TFA; flow, 1.4 mL/min; temperature 40 °C): 1.78 min, purity 99%. t_R (Waters XBridge C18, 2.5 μm , 3 mm \times 50 mm, 10–98% $\text{CH}_3\text{CN}-\text{H}_2\text{O}$ /8.6 min, 98% CH_3CN /1.4 min, CH_3CN and H_2O containing 0.1% TFA; flow, 1.4 mL/min; temperature 40 °C): 3.50 min, purity 99%. $[\alpha]_D^{20} -11.1$ ($c = 1.15$, MeOH). HRMS calcd for $\text{C}_{27}\text{H}_{39}\text{N}_2\text{O}_4$ $[\text{M} + \text{H}]^+$, 455.2904; found, 455.2905.

N-((3*R*,4*R*)-4-Benzylpyrrolidin-3-ylmethyl)-*N*-isopropyl-4-methoxy-3-(3-methoxypropoxy)benzamide, (3*R*,4*R*)-**12b**. The title compound was prepared in two steps as described for (*rac*)-**12** from (3*R*,4*S*)-**19b**. t_R (Waters XBridge C18, 2.5 μm , 3 mm \times 30 mm, 10–98% $\text{CH}_3\text{CN}/\text{H}_2\text{O}$ /3 min, 98% CH_3CN /0.5 min, CH_3CN and H_2O containing 0.1% TFA; flow, 1.4 mL/min; temperature 40 °C): 1.78 min, purity 99%. t_R (Waters XBridge C18, 2.5 μm , 3 mm \times 50 mm, 10–98% $\text{CH}_3\text{CN}-\text{H}_2\text{O}$ /8.6 min, 98% CH_3CN /1.4 min, CH_3CN and H_2O containing 0.1% TFA; flow, 1.4 mL/min; temperature 40 °C): 3.50 min, purity 100%. $[\alpha]_D^{20} +10.6$ ($c = 0.95$, MeOH). HRMS calcd for $\text{C}_{27}\text{H}_{39}\text{N}_2\text{O}_4$ $[\text{M} + \text{H}]^+$, 455.2904; found, 455.2904.

■ ASSOCIATED CONTENT

Supporting Information

Description of the 3D pharmacophore searching protocol, experimental procedures for biological assays, in vivo pharmacokinetics, in vivo pharmacology, X-ray crystallographic information for the rh-renin–inhibitor complexes with **5**, **6a**, and **12a**, X-ray crystal structure of two ligands *trans*-3,4-pyrrolidine **6a** bound to the active site of glycosylated rh-renin. This material is available free of charge via the Internet at <http://pubs.acs.org>.

Accession Codes

The crystal structures of rh-renin in complex with **5**, **6a**, and **12a** have been deposited at the Protein Data Bank RSCB PDB with the PDB IDs 4GJ5, 4GJ6, and 4GJ7, respectively.

■ AUTHOR INFORMATION

Corresponding Author

*For E.L.: phone, +41-61-6961955; fax, +41-61-6967155; E-mail, edwige.lorthois@novartis.com. For J.M.: phone, +41-61-6965560; fax, +41-61-6967155; E-mail, juergen_klaus.maibaum@novartis.com.

Present Address

[†]Novartis Institutes for BioMedical Research, Horsham, West Sussex RH12 5AB, UK.

Notes

The authors declare no competing financial interest.

■ ACKNOWLEDGMENTS

We thank Anne Rogemont, Jean-Francois Bulber, and Florence Zink for excellent technical assistance and Hans-Peter Baum and Markus Sanner for IC₅₀ determinations. We are grateful to Gabrielle Lecis and Claude Hager for chiral separations and to Markus Krömer for X-ray data depositions.

■ ABBREVIATIONS USED

AngI, angiotensin I; AngII, angiotensin II; AT1 receptor, angiotensin I receptor; DRI, direct renin inhibitor; FRET, fluorescence resonance energy transfer; GRAB, group replacement assisted binding; HE, hydroxyethylene; RAAS, renin–angiotensin–aldosterone system; rh-renin, recombinant human renin; S3^{SP}, S3 subpocket; dTGR, double transgenic rats

■ REFERENCES

(1) Ezzi, M.; Lopez, A. D.; Rodgers, A.; Vander-Hoorn, S.; Murray, C. J. L. Selected major risk factors and global and regional burden of disease. *Lancet* **2002**, *360* (9343), 1347–1360.

(2) Scott, B. B.; McGeehan, G. M.; Harrison, R. R. Development of inhibitors of the aspartyl protease renin for the treatment of hypertension. *Curr. Protein Pept. Sci.* **2006**, *7*, 241–254.

(3) Nicholls, M. G.; Robertson, J. I. S.; Inagami, T. The renin–angiotensin system in the twenty-first century. *Blood Pressure* **2001**, *10*, 327–343.

(4) Castrop, H.; Höcherl, K.; Kurtz, A.; Schweda, F.; Todorov, V.; Wagner, C. Physiology of kidney renin. *Physiol. Rev.* **2010**, *90*, 607–673.

(5) Skeggs, L.; Kahn, J. R.; Lentz, K. E.; Shumway, N. P. Preparation, purification and amino acid sequence of a polypeptide renin substrate. *J. Exp. Med.* **1957**, *106*, 439–453.

(6) Jackson, E. K. Renin and Angiotensin. In *Goodman and Gilman's: The Pharmacological Basis of Therapeutics*, 11th ed.; Brunton, L., Lazo, J., Parker, K., Buxton, I., Blumenthal, D., Eds.; McGraw-Hill: New York, 2006; pp 789–821.

(7) Mehta, P. K.; Griendling, K. K. Angiotensin II cell signaling: physiological and pathological effects in the cardiovascular system. *Am. J. Physiol. Cell Physiol.* **2007**, *292*, C82–C97.

(8) Wood, J. M.; Stanton, J. L.; Hofbauer, K. G. Inhibitors of renin as potential therapeutic agents. *J. Enzyme Inhib.* **1987**, *1*, 169–185.

(9) Fisher, N. D.; Hollenberg, N. K. Is there a future for renin inhibitors? *Expert Opin. Invest. Drugs* **2001**, *10*, 417–426.

(10) Ferro, A.; Gilbert, R.; Krum, H. Importance of renin in blood pressure regulation and therapeutic potential of renin inhibition. *Int. J. Clin. Pract.* **2006**, *60*, 577–581.

(11) Cheng, H.; Harris, R. C. Potential side effects of renin inhibitors—mechanisms based on comparison with other renin–angiotensin blockers. *Expert Opin. Drug Safety* **2006**, *5*, 631–641.

(12) Azizi, M.; Menard, J. Combined blockade of the renin–angiotensin system with angiotensin-converting enzyme inhibitors and angiotensin II type 1 receptor antagonists. *Circulation* **2004**, *109*, 2492–2499.

(13) (a) Karlberg, B. E. Cough and inhibition of the renin–angiotensin system. *J. Hypertens.* **1993**, *11* (Suppl), S49–S52.

(b) Cugno, M.; Nussberger, J.; Cicardi, M.; Agostoni, A. Bradykinin and the pathophysiology of angioedema. *Int. Immunopharmacol.* **2003**, *3*, 311–317.

(14) Parving, H. H.; Persson, F.; Lewis, J. B.; Lewis, E. J.; Hollenberg, N. K. Aliskiren combined with losartan in type 2 diabetes and nephropathy. *N. Engl. J. Med.* **2008**, *358*, 2433–2445.

(15) Webb, R. L.; Schiering, N.; Sedrani, R.; Maibaum, J. Direct Renin Inhibitors as A New Therapy for Hypertension. *J. Med. Chem.* **2010**, *53*, 7490–7520.

(16) Tice, C. M. and Singh S. B. Evolution of Diverse Classes of Renin Inhibitors through the Years. In *Aspartic Acid Proteases as Therapeutic Targets*, Ghosh, A. K., Ed.; Methods and Principles in Medicinal Chemistry, Mannhold, R., Kubinyi, H., Folkers, G., Eds.; Wiley-VCH: Weinheim, Germany, **2010**, Vol. 45, pp 297–324.

(17) (a) Wood, J. M.; Maibaum, J.; Rahuel, J.; Grütter, M. G.; Cohen, N.-C.; Rasetti, V.; Rüeger, H.; Göschke, R.; Stutz, S.; Fuhrer, W.; Schilling, W.; Rigollier, P.; Yamaguchi, Y.; Cumin, F.; Baum, H.-P.; Schnell, C. R.; Herold, P.; Mah, R.; Jensen, C.; O'Brien, E.; Stanton, A.; Bedigian, M. P. Structure-based design of aliskiren, a novel orally effective renin inhibitor. *Biochem. Biophys. Res. Commun.* **2003**, *308*, 698–705. (b) Maibaum, J.; Stutz, S.; Göschke, R.; Rigollier, P.; Yamaguchi, Y.; Cumin, F.; Rahuel, J.; Baum, H.-P.; Cohen, N.-C.; Schnell, C. R.; Fuhrer, W.; Grütter, M. G.; Schilling, W.; Wood, J. M. *J. Med. Chem.* **2007**, *50*, 4832–4844.

(18) Maibaum, J.; Feldman, D. L. Case history on Tekturna/Rasilez (aliskiren), a highly efficacious direct oral renin inhibitor as a new therapy for hypertension. *Annu. Rev. Med. Chem.* **2009**, *44*, 105–127.

(19) Bursavich, M. G.; Rich, D. H. Designing non-peptide peptidomimetics in the 21st century: inhibitors targeting conformational ensembles. *J. Med. Chem.* **2002**, *45*, 541–558.

(20) Oefner, C.; Binggeli, A.; Breu, V.; Bur, D.; Clozel, J.-P.; D'Arcy, A.; Dorn, A.; Fischli, W.; Grüniger, F.; Güller, R.; Märki, H. P.; Mathews, S.; Müller, M.; Ridley, R. G.; Stadler, H.; Vieira, E.; Wilhelm, M.; Winkler, F. K.; Wostl, W. *Chem. Biol.* **1999**, *6*, 127–131 The X-ray

structure for the disclosed GRAB peptidomimetic inhibitor 2-chlorobenzoic acid 4-[(3*S*,4*R*,5*R*)-3-methoxymethyl-5-(naphthalen-2-ylmethoxy)-piperidin-4-yl]-benzyl ester in complex with recombinant human renin (PDB code 1PR8) had been made publicly available by the Protein Data Bank during a restricted time period. This data has been retracted in the meantime for unknown reasons.

(21) Märki, H. P.; Binggeli, A.; Bittner, B.; Bohner-Lang, V.; Breu, V.; Bur, D.; Coassolo, Ph.; Clozel, J. P.; D'Arcy, A.; Doebeli, H.; Fischli, W.; Funk, Ch.; Foricher, J.; Giller, T.; Grüniger, F.; Guenzi, A.; Güller, R.; Hartung, T.; Hirth, G.; Jenny, Ch.; Kansy, M.; Klinkhammer, U.; Lave, T.; Lohri, B.; Luft, F. C.; Mervaala, E. M.; Müller, D. N.; Müller, M.; Montavon, F.; Oefner, Ch.; Qiu, C.; Reichel, A.; Sanwald-Ducray, P.; Scalone, M.; Schleimer, M.; Schmid, R.; Stadler, H.; Treiber, A.; Valdenaire, O.; Vieira, E.; Waldmeier, P.; Wiegand-Chou, R.; Wilhelm, M.; Wostl, W.; Zell, M.; Zell, R. Piperidine renin inhibitors: from leads to drug candidates. *Farmaco* **2001**, *56*, 21–27.

(22) (a) Bezencon, O.; Bur, D.; Weller, T.; Richard-Bildstein, S.; Remeň, L.; Sifferlen, T.; Corminboeuf, O.; Grisostomi, C.; Boss, C.; Prade, L.; Delahye, S.; Treiber, A.; Strickner, P.; Binkert, C.; Hess, P.; Steiner, B.; Fischli, W. Design and preparation of potent, nonpeptidic, bioavailable renin inhibitors. *J. Med. Chem.* **2009**, *52*, 3689–3702. (b) For the discovery of ACT-178882/MK-1597, see also Corminboeuf, O.; Bezencon, O.; Remeň, L.; Grisostomi, C.; Richard-Bildstein, S.; Bur, D.; Prade, L.; Strickner, P.; Hess, P.; Fischli, W.; Steiner, B.; Treiber, A. Piperidine-based renin inhibitors: upper chain optimization. *Bioorg. Med. Chem. Lett.* **2010**, *20*, 6291–6296.

(23) Kasai, A.; Subedi, R.; Stier, M.; Holsworth, D. D. Cardiovascular agents: renin inhibitors and factor Xa inhibitors. *Heterocycles* **2007**, *73*, 47–85.

(24) Jia, L.; Simpson, R. D.; Yuan, J.; Xu, Z.; Zhao, W.; Cacatian, S.; Tice, C. M.; Guo, J.; Ishchenko, A.; Singh, S. B.; Wu, Z.; McKeever, B. M.; Bukhtiyarov, Y.; Johnson; Judith, A.; Doe, C. P.; Harrison, R. K.; McGeehan, G. M.; Dillard, L. W.; Baldwin, J. J.; Claremon, D. A. Discovery of VTP-27999, an Alkyl Amine Renin Inhibitor with Potential for Clinical Utility. *ACS Med. Chem. Lett.* **2011**, *2*, 747–751.

(25) Ostermann, N.; Ruedisser, S.; Ehrhardt, C.; Breitenstein, W.; Marzinzik, A.; Jacoby, E.; Vangrevelinghe, E.; Ottl, J.; Klumpp, M.; Hartweg, J. C. D.; Cumin, F.; Hassiwen, U.; Trappe, J.; Sedrani, R.; Geisse, S.; Gerhartz, B.; Richert, P.; Francotte, E.; Wagner, T.; Krömer, M.; Kosaka, T.; Webb, R. L.; Rigel, D. F.; Maibaum, J.; Baeschlin, D. K. A novel class of oral direct renin inhibitors: highly potent 3,5-disubstituted piperidines bearing a tricyclic P₃-P₁ pharmacophore. *J. Med. Chem.* **2013**, *56*, DOI: 10.1021/jm301706j.

(26) (a) See Supporting Information. (b) See Experimental Section. (c) X-ray crystal structure of two ligands trans-3,4-pyrrolidine **6a** bound to the active site of glycosylated rh-renin, see Supporting Information.

(27) Compound **5**, available from the Novartis Collection, has been described as inhibitor of aspartyl protease by Bursavich, M. G.; Rich, D. H. Solid-Phase Synthesis of Aspartic Peptidase Inhibitors: 3-Alkoxy-4-Aryl Piperidines. *Org. Lett.* **2001**, *3*, 2625–2628.

(28) Rahuel, J.; Rasetti, V.; Maibaum, J.; Rüeger, H.; Göschke, R.; Cohen, N.-C.; Stutz, S.; Cumin, F.; Fuhrer, W.; Wood, J. M.; Grütter, M. G. Structure-based drug design: the discovery of novel nonpeptide orally active inhibitors of human renin. *Chem. Biol.* **2000**, *7*, 493–504.

(29) Yamaguchi, Y.; Menear, K.; Cohen, N.-C.; Mah, R.; Cumin, F.; Schnell, C.; Wood, J. M.; Maibaum, J. The P1 N-isopropyl motif bearing hydroxyethylene dipeptide isostere analogs of aliskiren are in vitro potent inhibitors of the human aspartyl protease renin. *Bioorg. Med. Chem. Lett.* **2009**, *19*, 4863–4867.

(30) Göschke, R.; Cohen, N.-C.; Wood, J. M.; Maibaum, J. Design and synthesis of novel 2,7-dialkyl substituted 5(*S*)-amino-4(*S*)-hydroxy-8-phenyl-octanecarboxamides as in vitro potent peptidomimetic inhibitors of human renin. *Bioorg. Med. Chem. Lett.* **1997**, *7*, 2735–2740.

(31) Specker, E.; Böttcher, J.; Brass, S.; Heine, A.; Lilie, H.; Schoop, A.; Müller, G.; Griebenow, N.; Klebe, G. Unexpected novel binding mode of pyrrolidine-based aspartyl protease inhibitors: design,

synthesis and crystal structure in complex with HIV protease. *ChemMedChem* **2006**, *1*, 106–117.

(32) Chen, A.; Campeau, L.-C.; Cauchon, E.; Chefson, A.; Ducharme, Y.; Dubé, D.; Falguyret, J.-P.; Fournier, P.-A.; Gagné, S.; Grimm, E.; Han, Y.; Houle, R.; Huang, J.-Q.; Lacombe, P.; Laliberté, S.; Lévesque, J.-F.; Liu, S.; MacDonald, D.; Mackay, B.; McKay, D.; Percival, M. D.; Regan, C.; Regan, H.; St-Jacques, R.; Toulmond, S. Renin inhibitors for the treatment of hypertension: Design and optimization of a novel series of pyridone-substituted piperidines. *Bioorg. Med. Chem. Lett.* **2011**, *21*, 3970–3975.

(33) Scheiper, A.; Matter, H.; Steinhagen, H.; Stütz, U.; Böcskei, Z.; Fleury, V.; McCort, G. Discovery and optimization of a new class of potent and non-chiral indole-3-carboxamide-based renin inhibitors. *Bioorg. Med. Chem. Lett.* **2010**, *20*, 6268–6272.

(34) Müller, G. Target Family-Directed Masterkeys in Chemogenomics. In *Chemogenomics in Drug Discovery: A Medicinal Chemistry Perspective*; Kubinyi, H.; Müller, G., Eds.; Wiley-VCH: Weinheim, Germany, 2004; pp 7–41.

(35) Stachel, S. J.; Steele, T. G.; Petrocchi, A.; Haugabook, S. J.; McGaughey, G.; Holloway, M. K.; Allison, T.; Munshi, S.; Zuck, P.; Colussi, D.; Tugasheva, K.; Wolfe, A.; Graham, S. L.; Vacca, J. P. Discovery of pyrrolidine-based- β -secretase inhibitors: lead advancement through conformational design for maintenance of ligand binding efficiency. *Bioorg. Med. Chem. Lett.* **2012**, *22*, 240–244. For an account on spiropyrrolidine Bace-1 inhibitors, see: Efremov, I. V.; Vajdos, F. F.; Borzilleri, K. A.; Capetta, S.; Chen, H.; Dorff, P. H.; Dutra, J. K.; Goldstein, S. W.; Mansour, M.; McColl, A.; Noell, S.; Oborski, C. E.; O'Connell, T. N.; O'Sullivan, T. J.; Pandit, J.; Wang, H.; Wei, B.; Withka, J. M. *J. Med. Chem.* **2012**, *55*, 9069–9088.

(36) *trans*-3,4-Disubstituted proline derivatives have been claimed as renin inhibitors, however, no experimental data on their binding mode to human renin has been disclosed to date. These compounds may interact with the flap binding pocket of renin in the open conformation in a similar manner as the piperidine-based GRAB peptidomimetic renin inhibitors represented by **2**, based on the close structural similarities of the extended pharmacophores at the C-4 position of the 5- and 6-membered ring core templates, respectively. Bezencon, O.; Boss, C.; Bur, D.; Corminboeuf, O.; Grisostomi, C.; Remen, L.; Richard-Bildstein, S.; Weller, T. PCT Int. Appl. WO2007034406A1, 2007.

(37) Bohlender, J.; Fukamizu, A.; Lippoldt, A.; Nomura, T.; Dietz, R.; Menard, J.; Murakami, K.; Luft, F. C.; Ganten, D. High human hypertension in transgenic rats. *Hypertension* **1997**, *29*, 428–434.

(38) (a) Hosomi, A.; Sakata, Y.; Sakurai, H. N-(Trimethylsilylmethyl)aminomethyl ethers as azomethine ylide synthons. A new and convenient access to pyrrolidine derivatives. *Chem. Lett.* **1984**, *7*, 1117–1120. (b) Terao, Y.; Kotaki, H.; Imai, N.; Achiwa, K. Trifluoroacetic acid-catalyzed 1,3-cycloaddition of the simplest iminium ylide leading to 3- or 3,4-substituted pyrrolidines and 2,5-dihydropyrroles. *Chem. Pharm. Bull.* **1985**, *33*, 2762–2766.

(39) Abdel-Magid, A. F.; Carson, K. G.; Harris, B. D.; Maryanoff, C. A.; Shah, R. D. Reductive amination of aldehydes and ketones with sodium triacetoxyborohydride. Studies on direct and indirect reductive amination procedures. *J. Org. Chem.* **1996**, *61*, 3849–3862.

(40) Breitenstein, W.; Cottens, S.; Ehrhardt, C.; Jacoby, E.; Lorthiois, E.; Maibaum, J.; Ostermann, N.; Sellner, H.; Simic, O. Preparation of Substituted Pyrrolidines as Renin Inhibitors. PCT Int. Appl. WO2006066896A2, 2006.

(41) Prashad, M.; Mak, X. Y.; Liu, Y.; Repic, O. Palladium-catalyzed amination of aryl bromides with hindered N-alkyl-substituted anilines using a palladium(I) tri-*tert*-butylphosphine bromide dimer. *J. Org. Chem.* **2003**, *68*, 1163–1164.